

(Cargèse, 7 June 2017)

"Imaging Earth's crust and mantle with scattered seismic waves"

R. van der Hilst¹

with M. de Hoop², M. Campillo^{1,3}, X.-F. Shang^{1,4}, C. Yu^{1,5}, L. Day^{1,6}

¹ Department of Earth, Atmospheric and Planetary Sciences
Massachusetts Institute of Technology

² Rice University

³ Univ. de Grenoble, France

⁴ Now at: Shell, Houston

⁵ Now at: Caltech

⁶ Now at: Imperial College, London

Research sponsored by

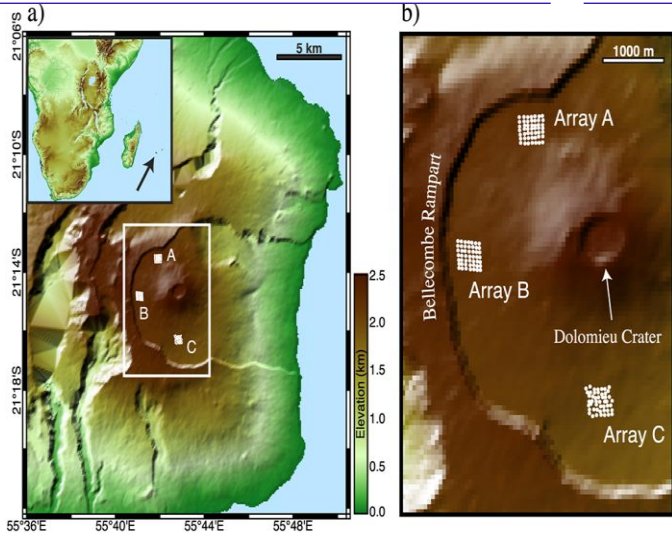




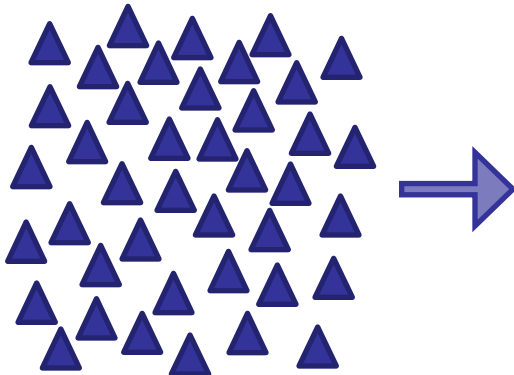
Noise-Based Measurements of Tidal- and Thermal-Induced Seismic Wave Speed Changes



Shujuan Mao¹, Michel Campillo^{1,2}, Robert van der Hilst¹, Florent Brenguer², Gregor Hillers², Laurent Stehly² (1) Massachusetts Institute of Technology, Department of Earth, Atmospheric and Planetary Sciences; (2) University Grenoble Alpes, ISTerre Institute of Earth Sciences

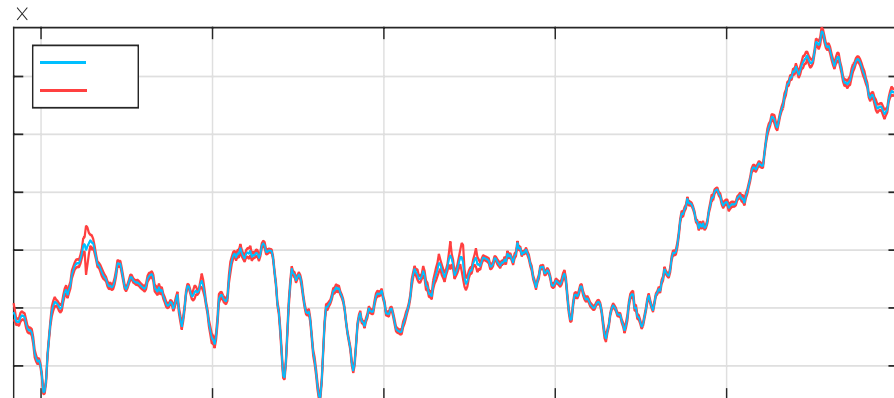
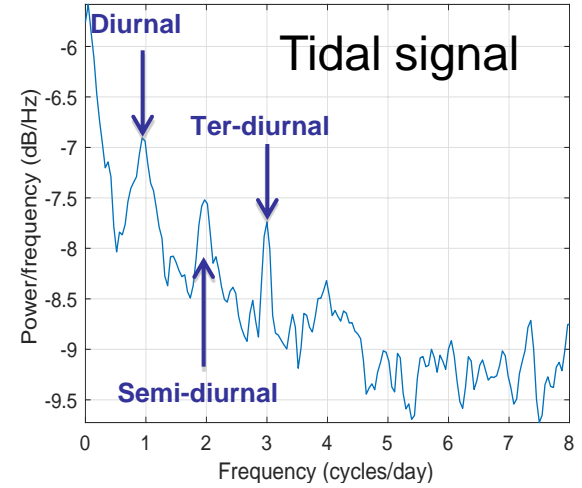


Large Dense Array



Poster by Shujuan Mao later this week

dv/v



Overview of lecture:

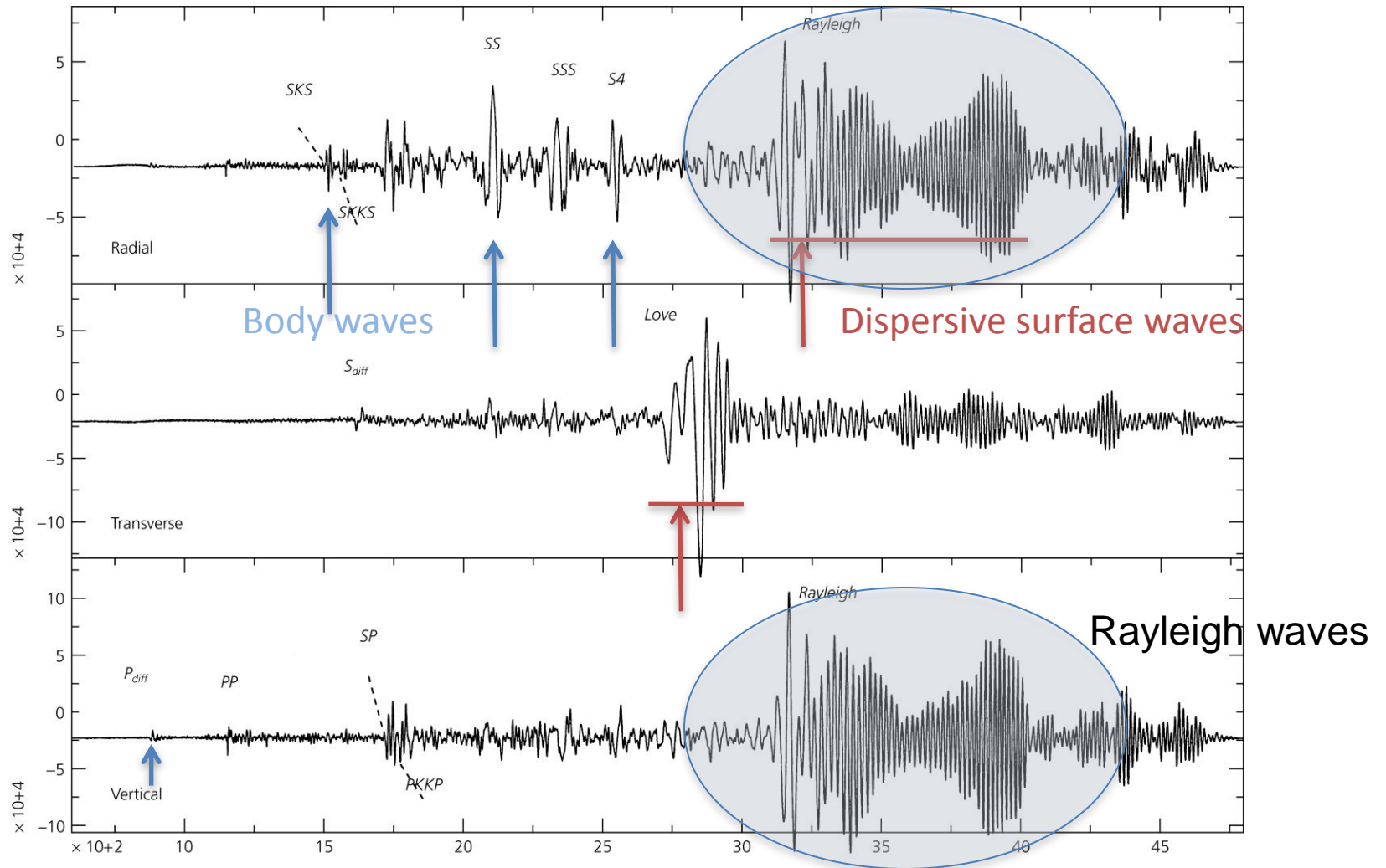
1. Introduction/background

2. Ambient noise and surface wave tomography (MIT, 2005-2015)

- combining ambient noise and earthquake data
- ~~➤ quantifying and correcting for uneven noise distribution~~
- ~~➤ azimuthal anisotropy~~
- radial anisotropy
- adjoint tomography with ambient noise data
- joint inversion dispersion data and receiver functions

3. Imaging of interfaces

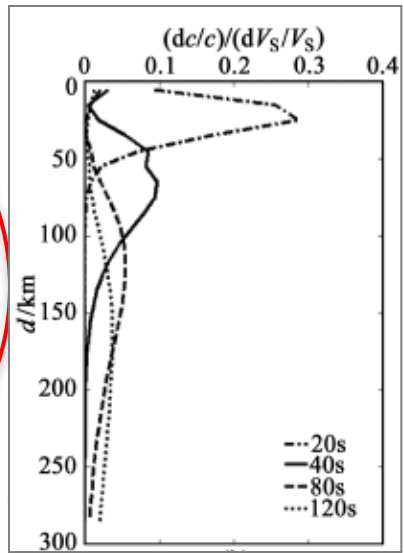
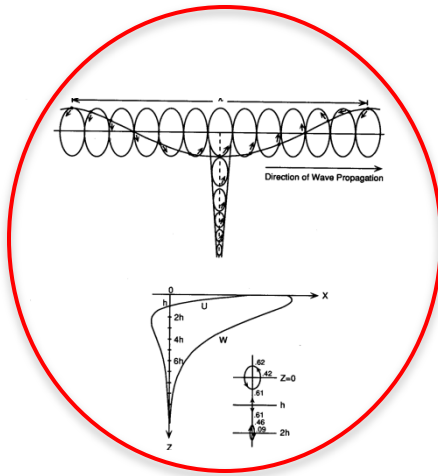
Figure 2.7-1: Seismograms recorded at a distance of 110°, showing surface waves.



From Stein and Wyession

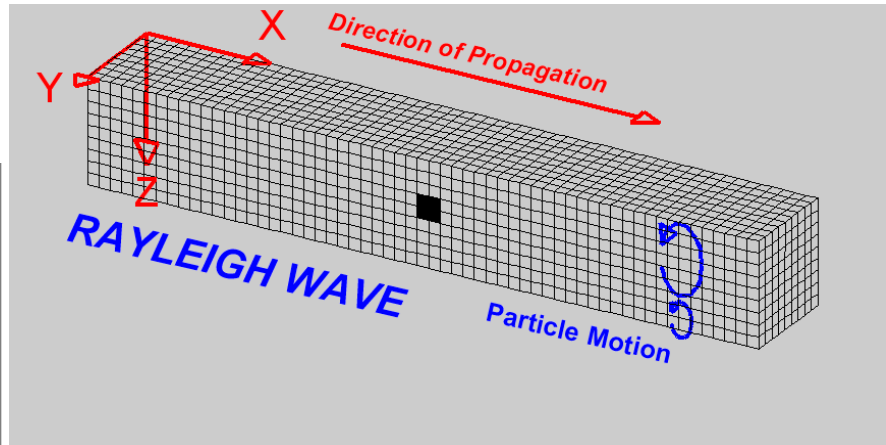
‘Surface and guided waves’: waves trapped in the shallow layers or a wave guide (such as Love waves in the Earth, acoustic waves in the oceanic SOFAR,)

space:



frequency proxy for depth

Rayleigh wave at the surface of an half-



Overview of lecture:

1. Introduction/background

2. Ambient noise and surface wave tomography (MIT, 2005-2015)

- combining ambient noise and earthquake data
- ~~➤ quantifying and correcting for uneven noise distribution~~
- ~~➤ azimuthal anisotropy~~
- radial anisotropy
- adjoint tomography with ambient noise data
- joint inversion dispersion data and receiver functions

3. Imaging of interfaces

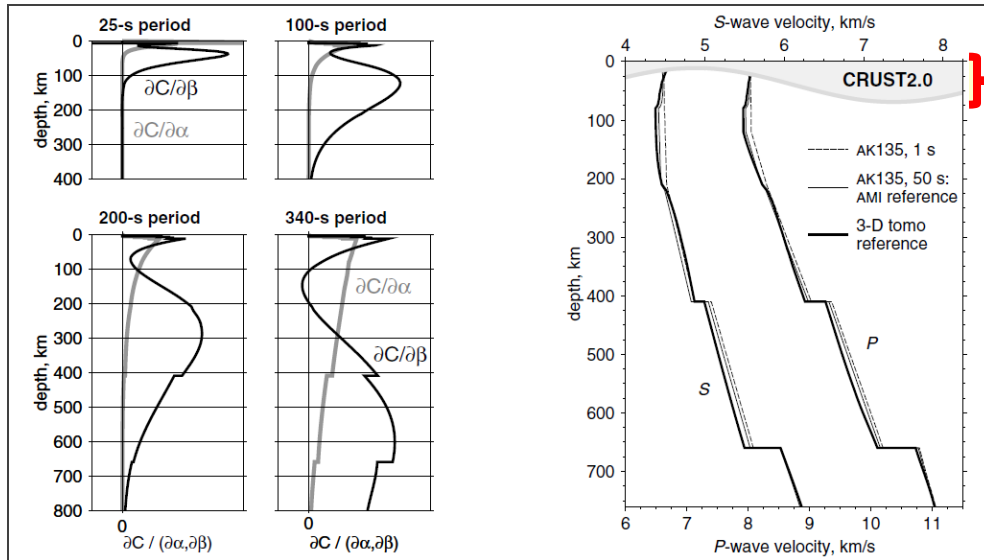
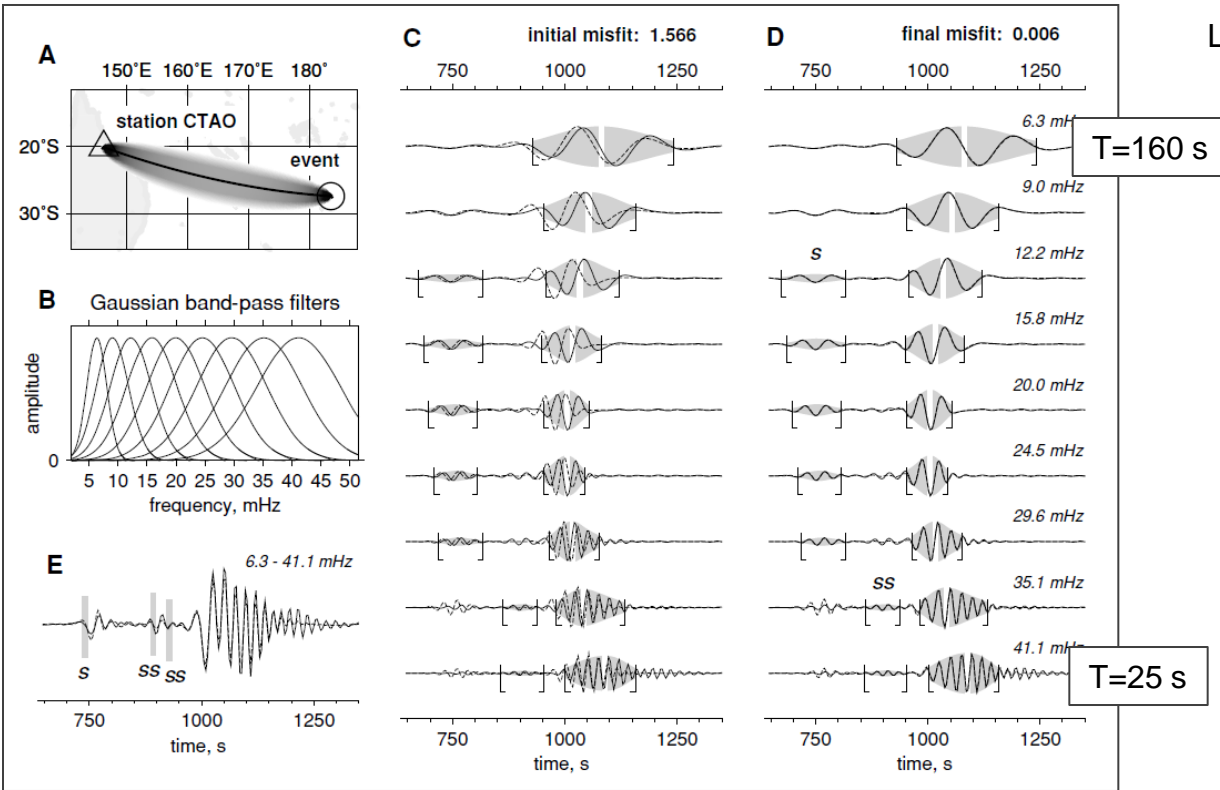
Traditional Approach to Tomography

DATA (Massive Sensor Networks;
Signal from Earthquakes)

**ballistic (source-to-receiver) wave
propagation**

Tomography
(Asymptotic or Full-Wave)
(Body waves, surface waves)

3-D Velocity Model that
best explains data

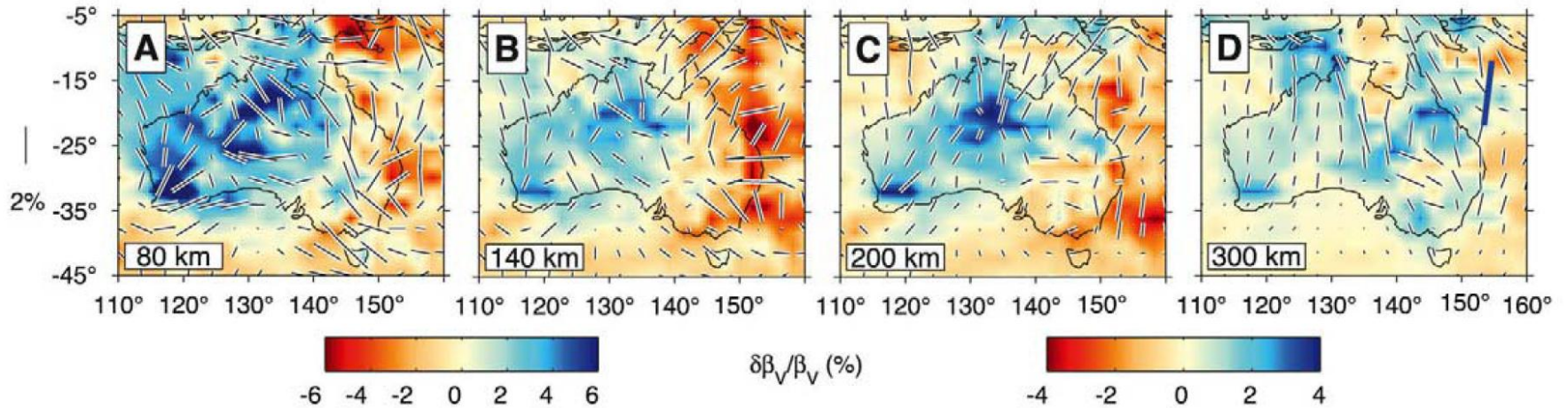


Crust = Problem!

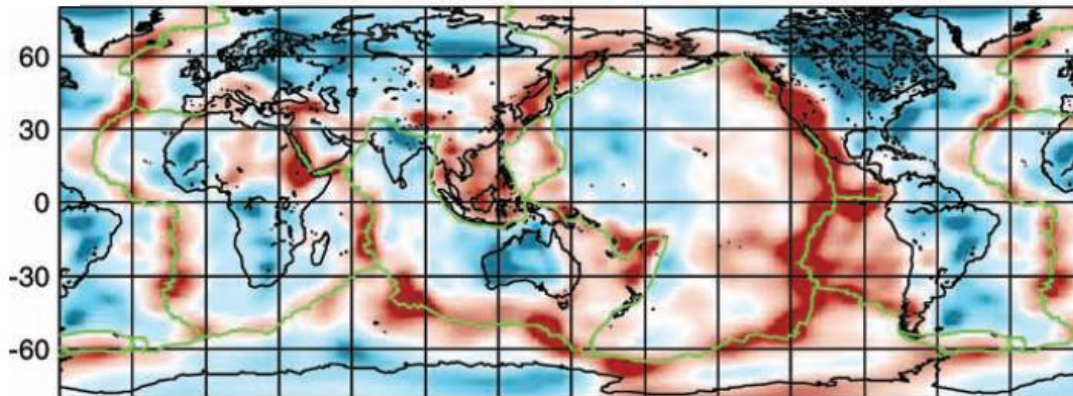
Examples from traditional surface wave tomography with earthquake waves: relatively low frequencies → deep structures

$T > 30 \text{ s} \rightarrow$ upper mantle

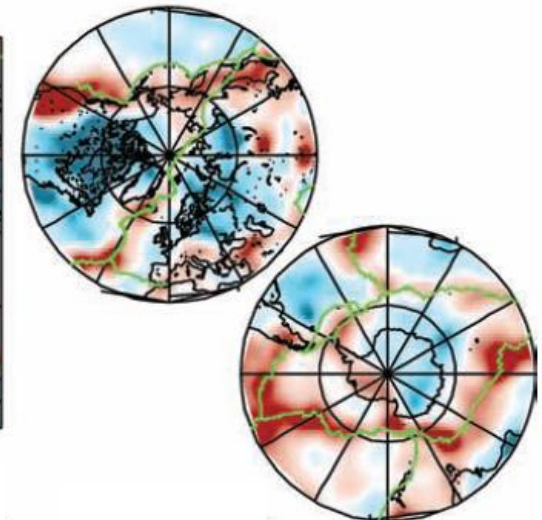
Simons and Van der Hilst (*EPSL*, 2003)



depth: 80 km



Lebedev and Van der Hilst (*GJI*, 2008)



Ambient Noise Tomography

DATA (Massive Sensor Networks;
background noise)

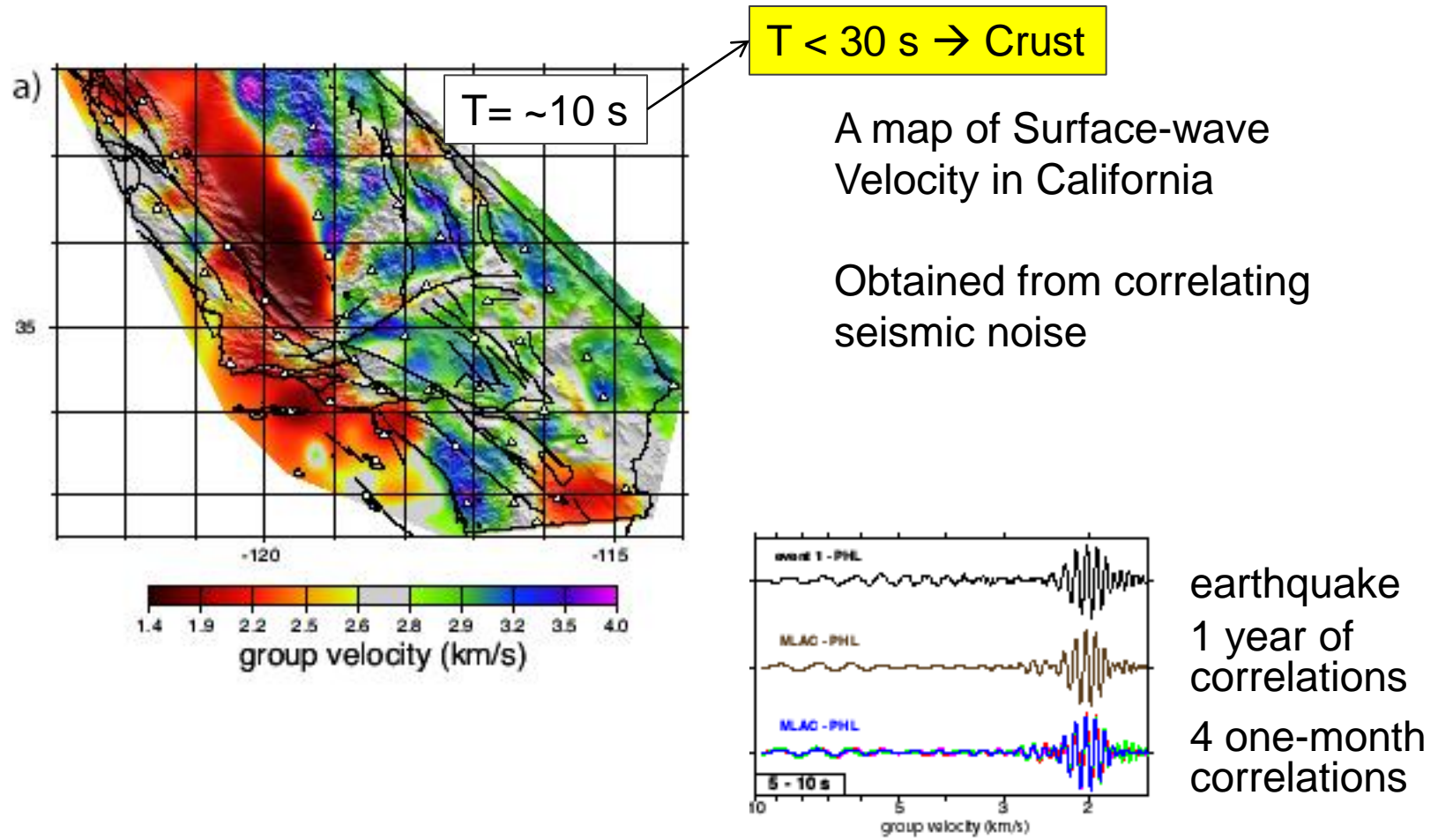
Alternative:
“sourceless” imaging/tomography

**create data by means of
interferometry/cross-correlation**

Tomography
(Asymptotic or Full-Wave)
(Body waves, surface waves)

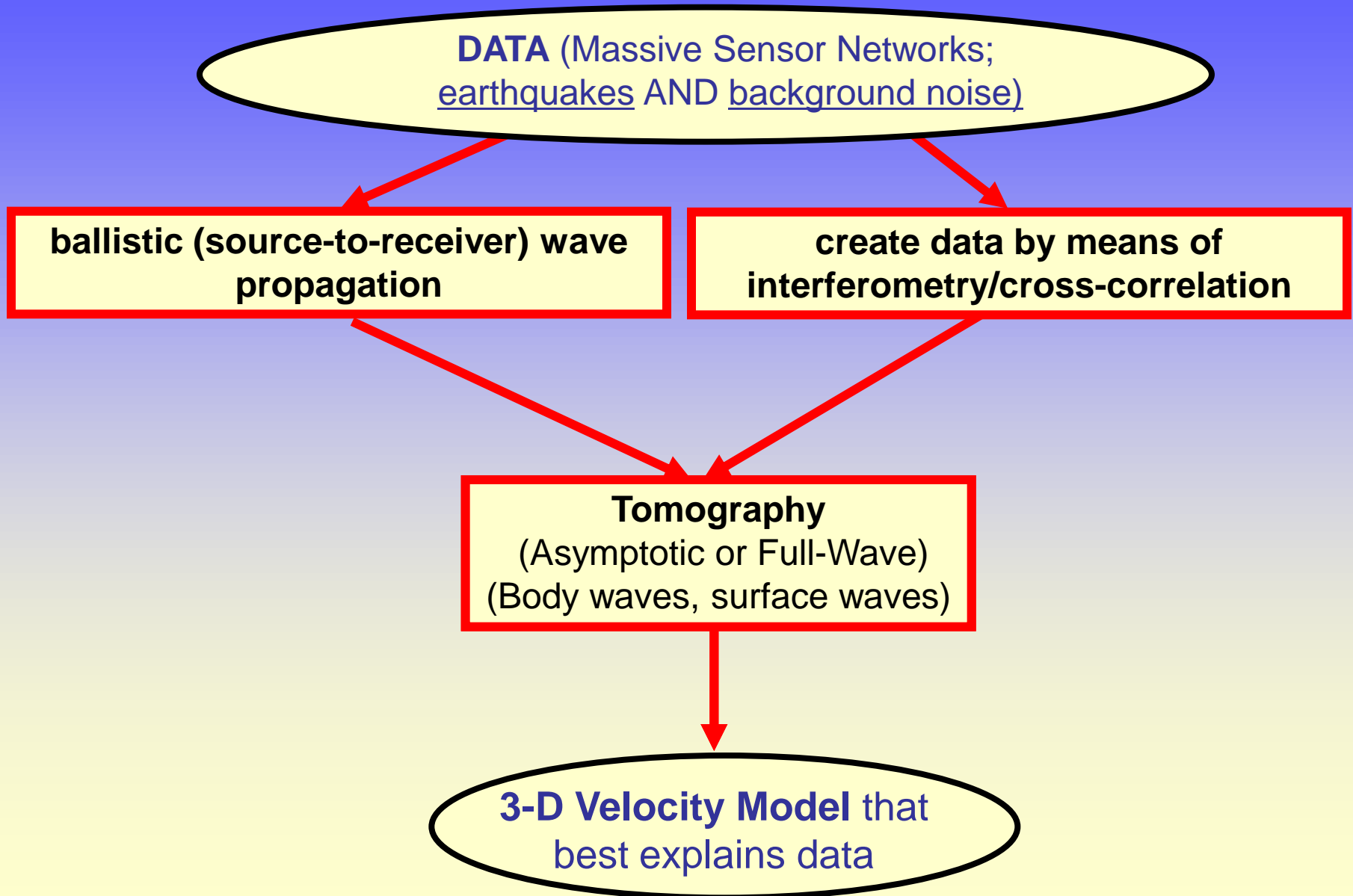
3-D Velocity Model that
best explains data

Shapiro, N.M., M. Campillo, L. Stehly, and M.H. Ritzwoller, 2005, High-Resolution Surface-Wave Tomography from Ambient Seismic Noise: *Science* **307**:1615-1618



also Sabra, et al Surface wave tomography from microseisms in Southern California
Geophys Res Lett **32** (2005)

Use both 'active' and 'passive' data



Field Projects Sichuan & Yunnan Provinces and E. Tibet (2003-2004)

Crust-Mantle study E Tibet – SW China



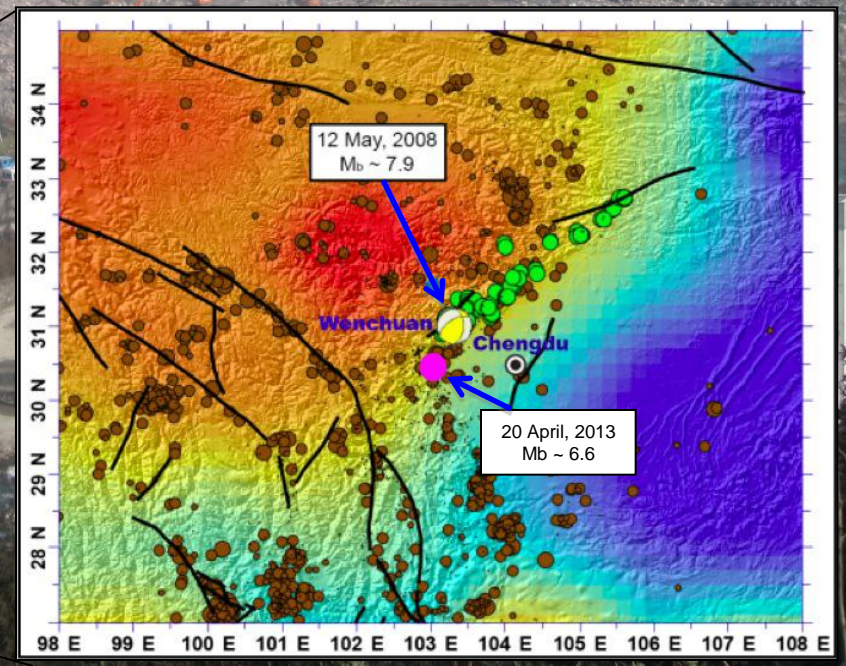
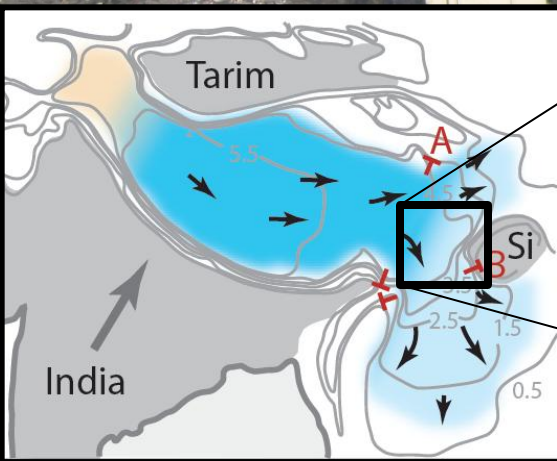
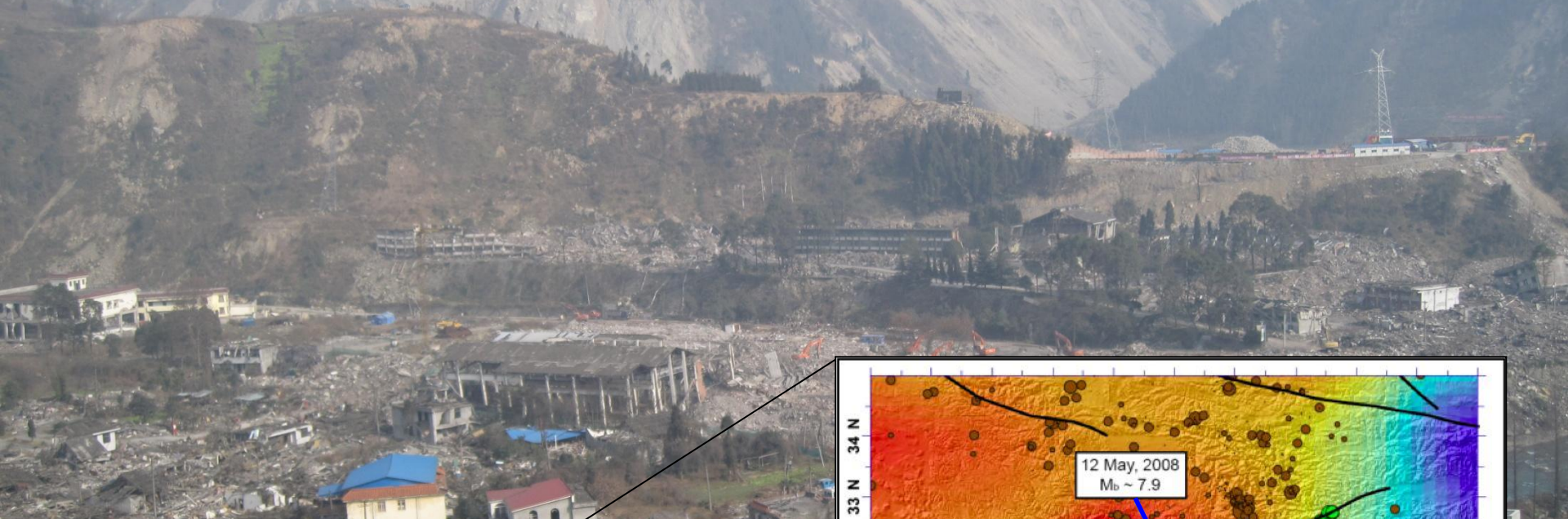
Why SE Tibet?

(Yingxiu, January 2009)

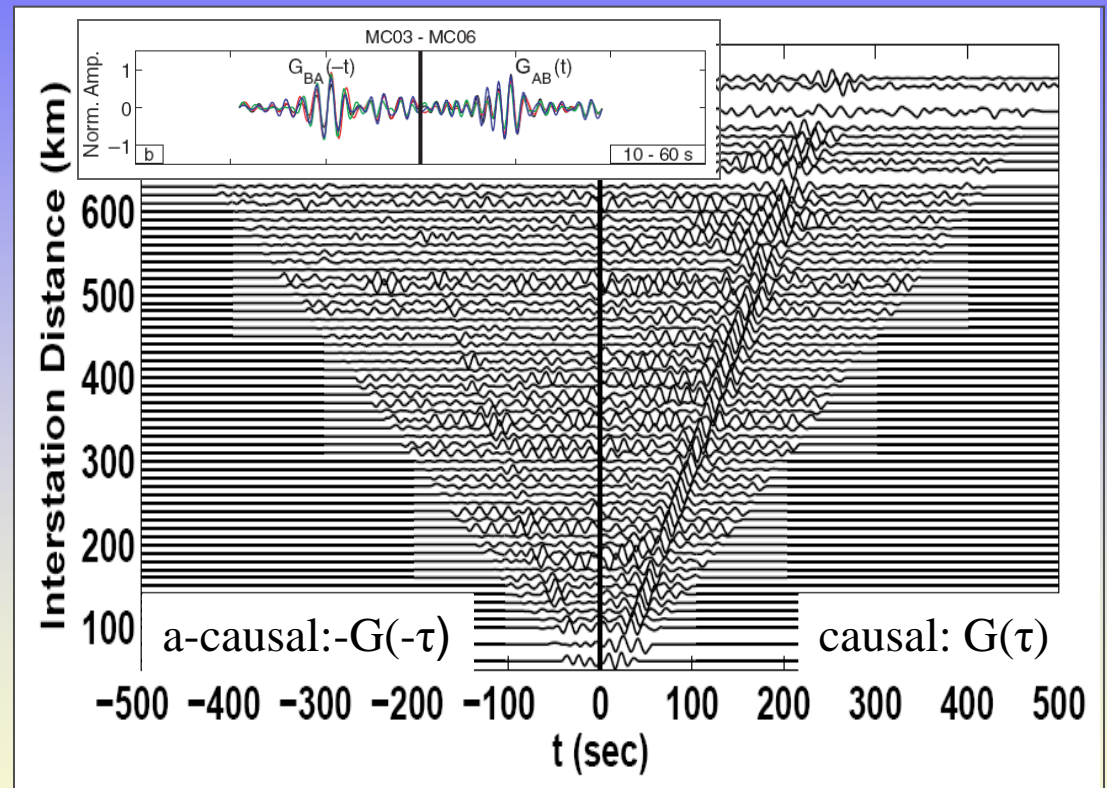
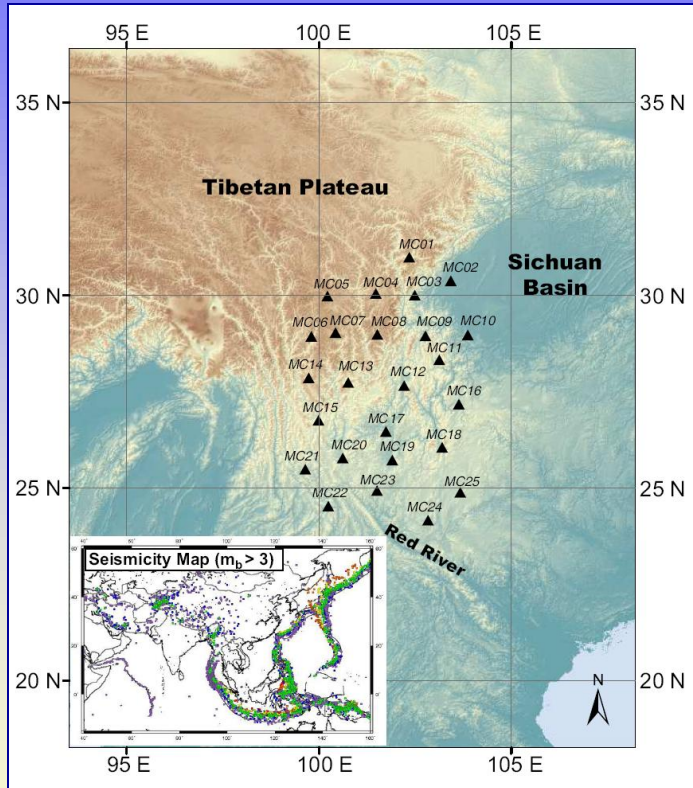
2. Southern end of Trans China Seismicity Belt

E.g. Sichuan, 12 May 2008

~80,000 people killed ...

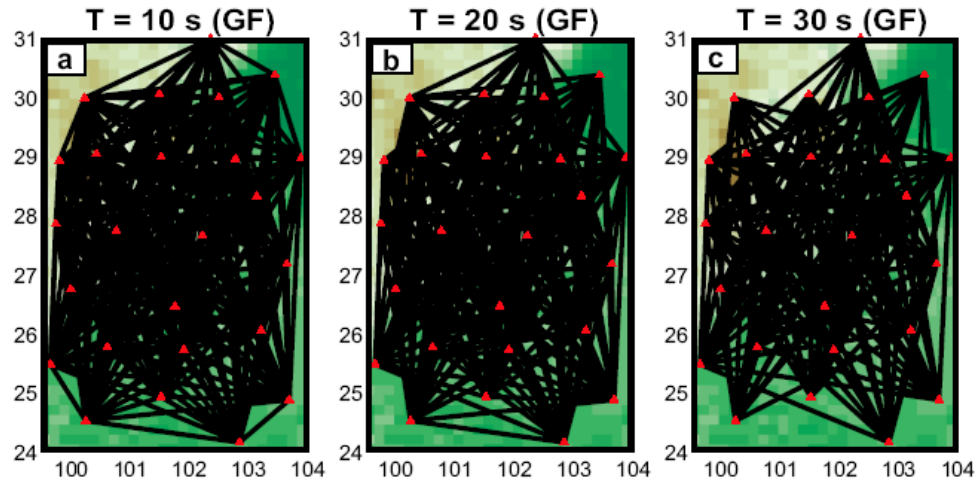


Crust and Lithosphere: Multi-resolution surface wave tomography



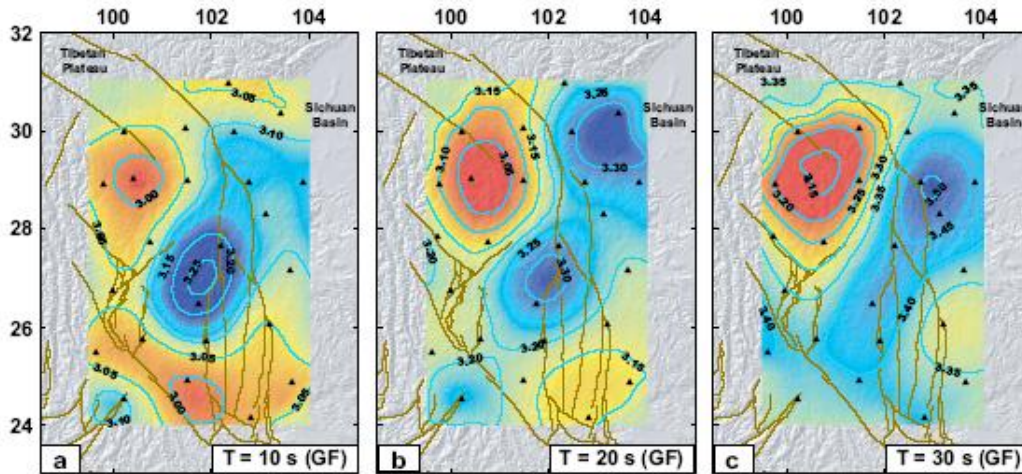
Seismic interferometry → estimate data from background “noise”
(NB we ignore asymmetry and sum causal and a-causal signals)

Example: “ambient noise” surface wave tomography



“source”-receiver pairs at different periods

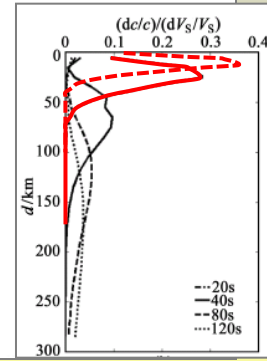
Example: “ambient noise” surface wave tomography



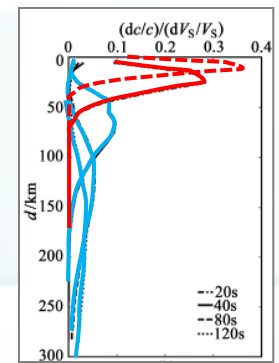
Phase velocity maps at different periods

Interferometry (scattering) → relatively short periods (high frequency)

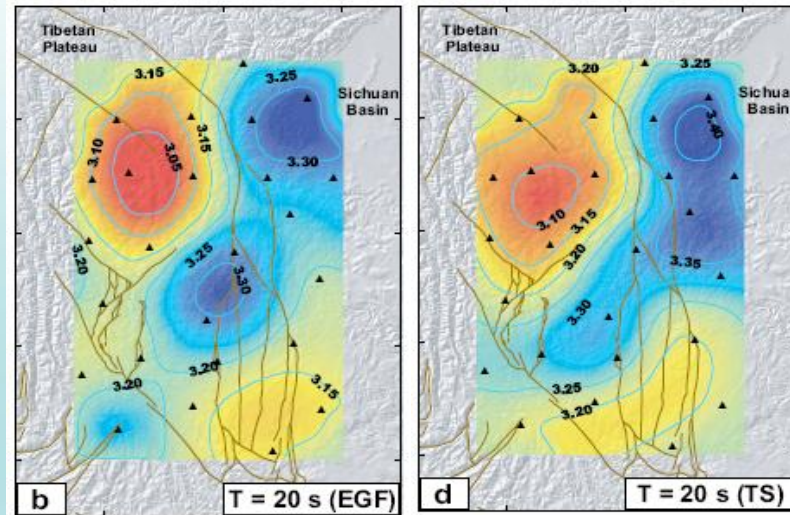
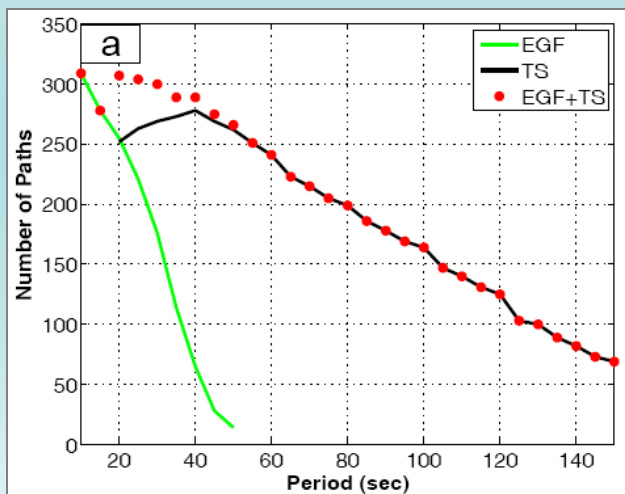
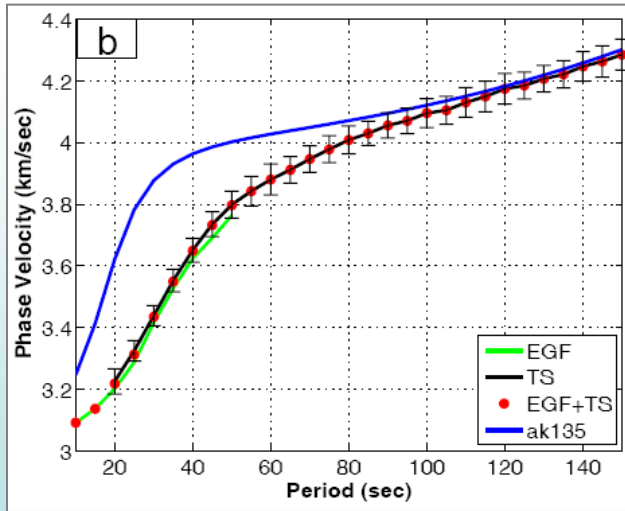
For surface wave tomography that means: “shallow” sub-surface



Combination of ambient noise and earthquake data: extend frequency range \rightarrow extend depth range

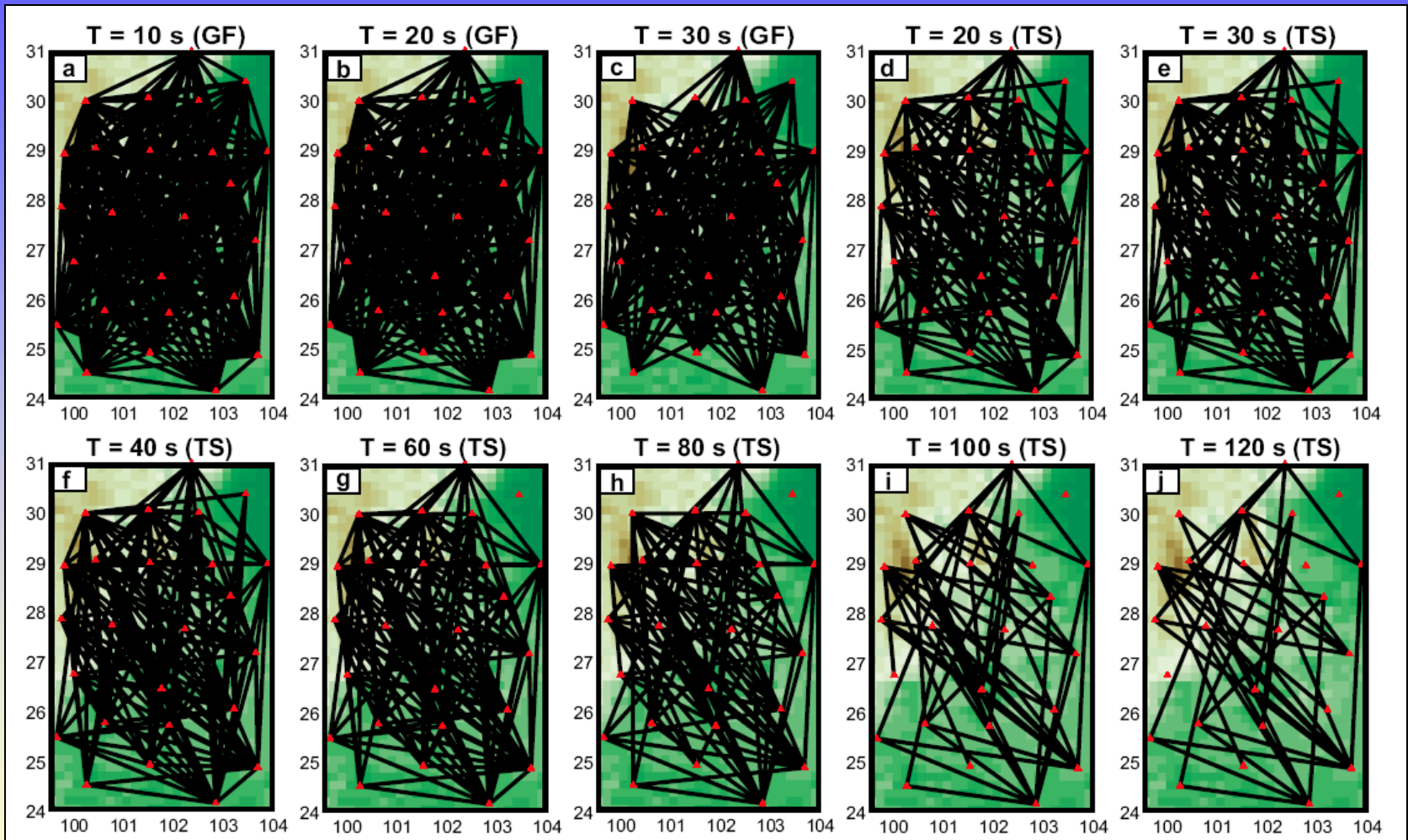


At overlapping periods, Rayleigh wave phase velocities from EGF (from 10 months Z-comp. data) and TS analyses are similar

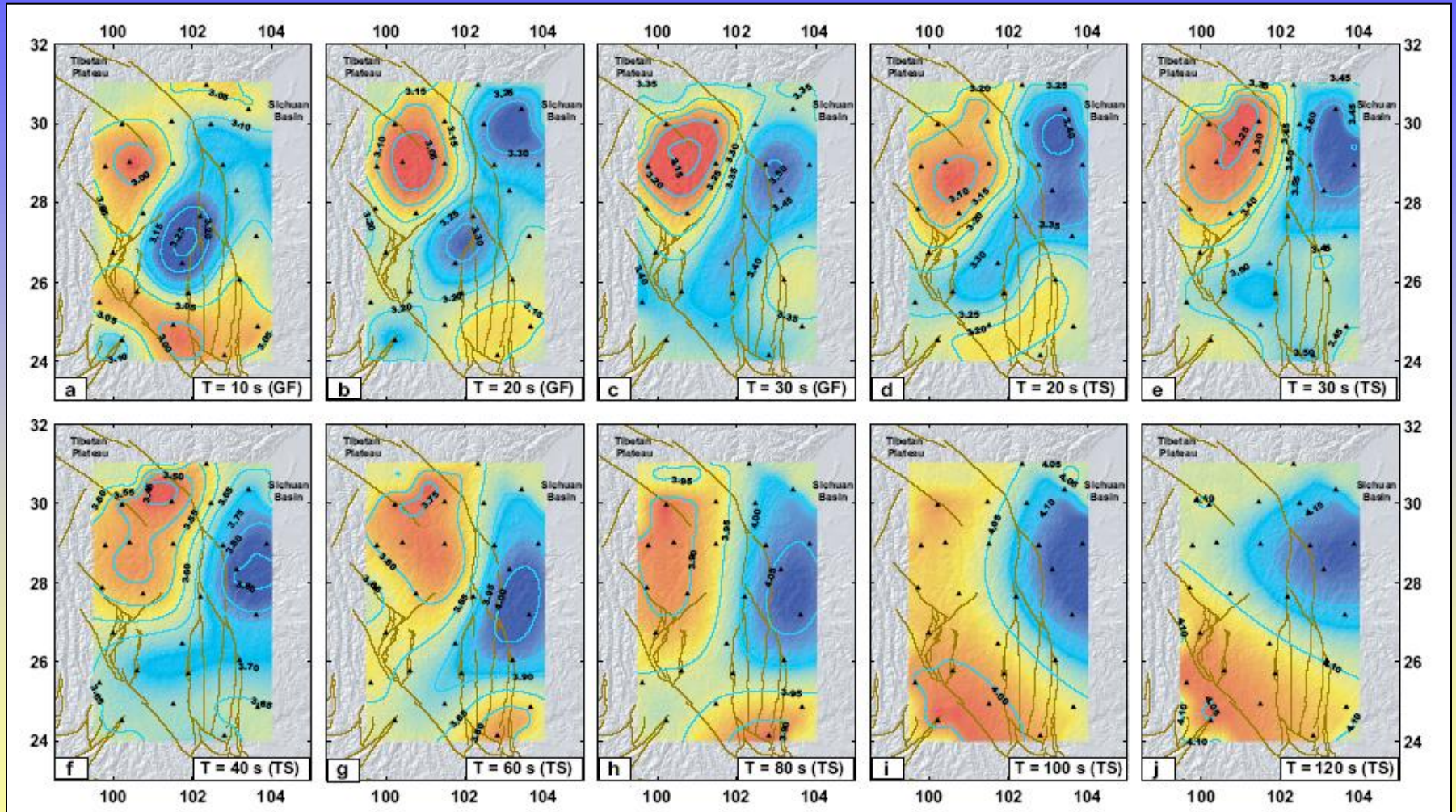


- TS slightly higher ($< 0.7\%$) due to differences in finite frequency effect
- Difference \ll medium perturbations ($< 10\%$)

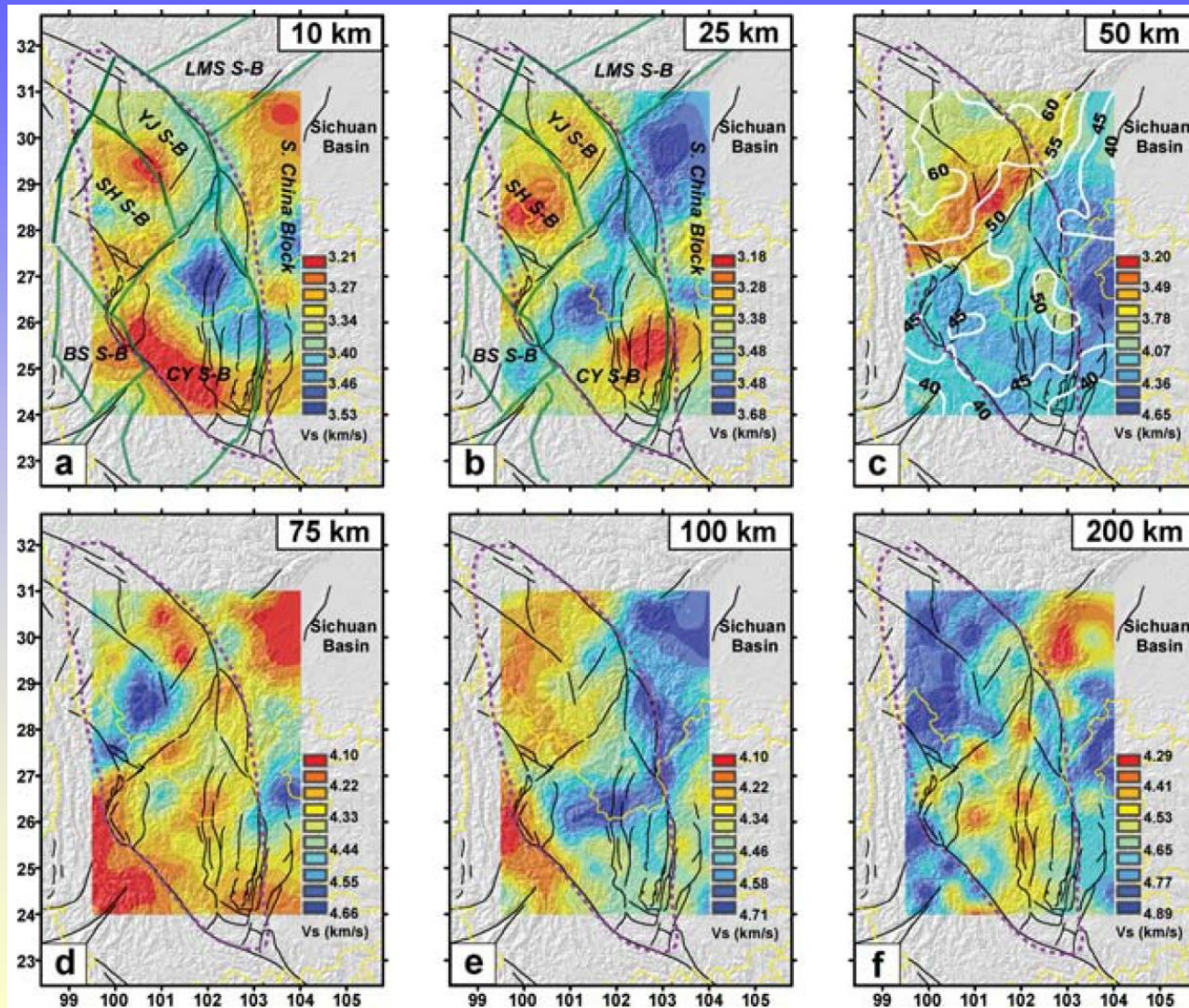
Multi-resolution surface wave tomography



Phase velocity maps at different periods



Multi-resolution surface wave tomography



Overview of lecture:

1. Introduction/background

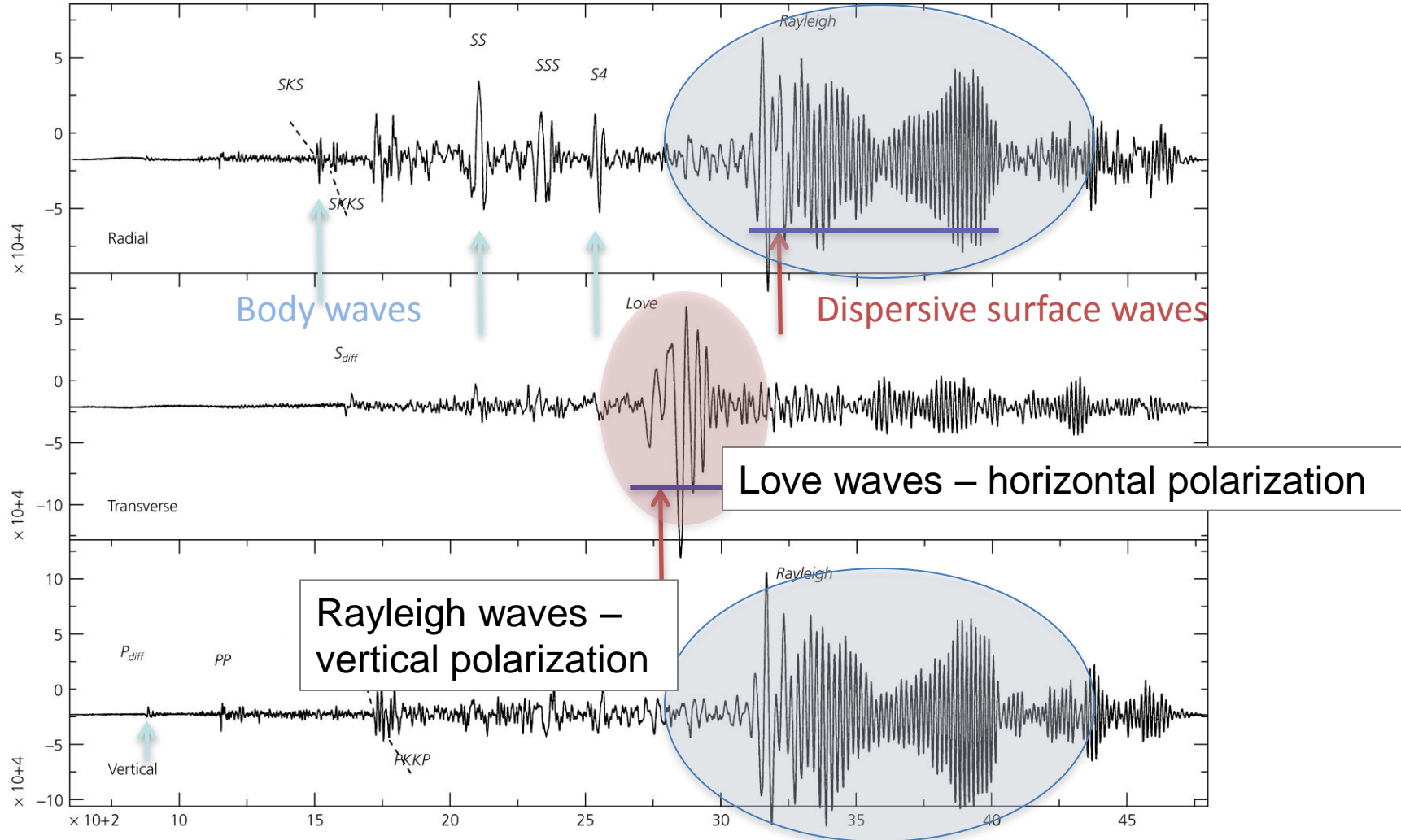
2. Ambient noise and surface wave tomography (MIT, 2005-2015)

- combining ambient noise and earthquake data
- ~~➤ quantifying and correcting for uneven noise distribution~~
- ~~➤ azimuthal anisotropy~~
- **radial anisotropy**
- adjoint tomography with ambient noise data
- joint inversion dispersion data and receiver functions

3. Imaging of interfaces

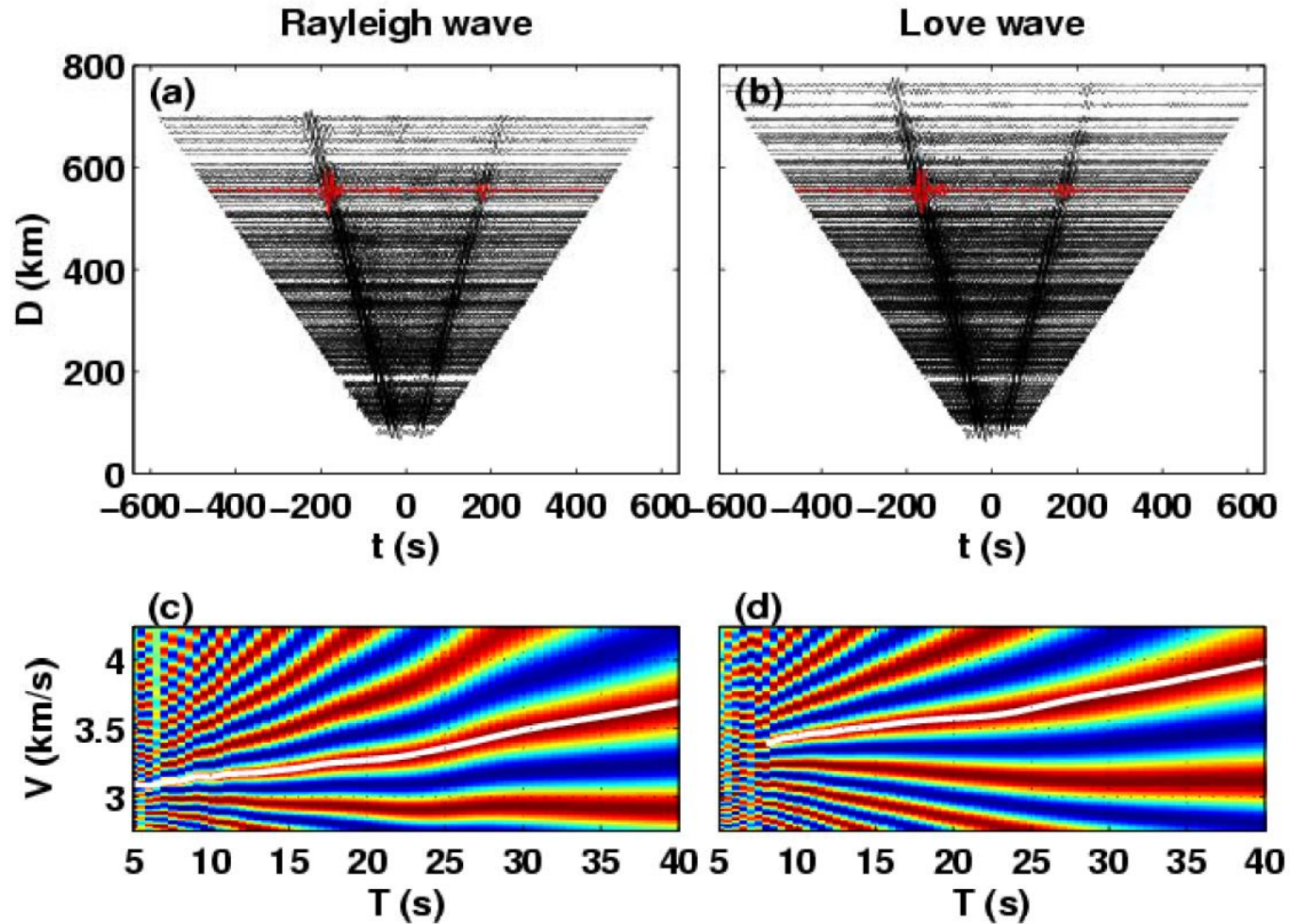
Anisotropy II: Radial Anisotropy (or: transverse isotropy)

(i.e., difference between wavespeed of horizontally and vertically polarized waves)



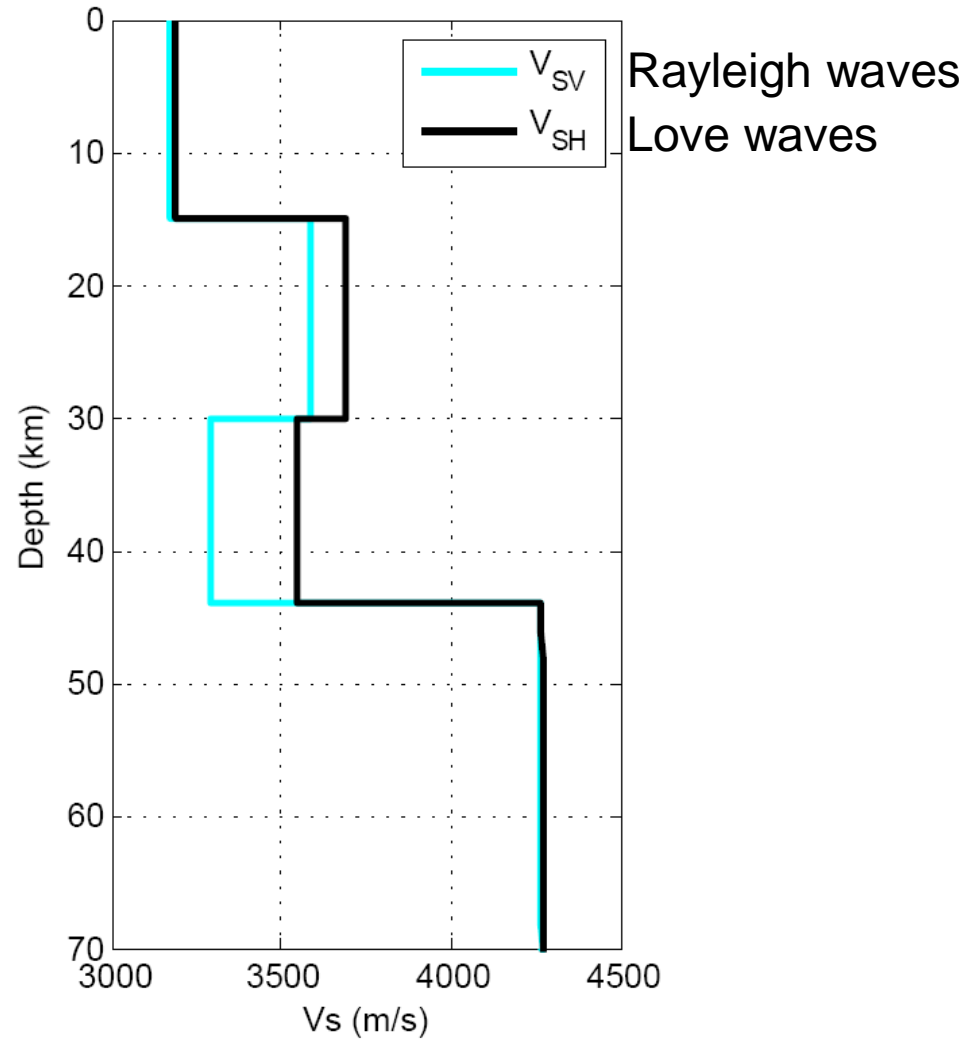
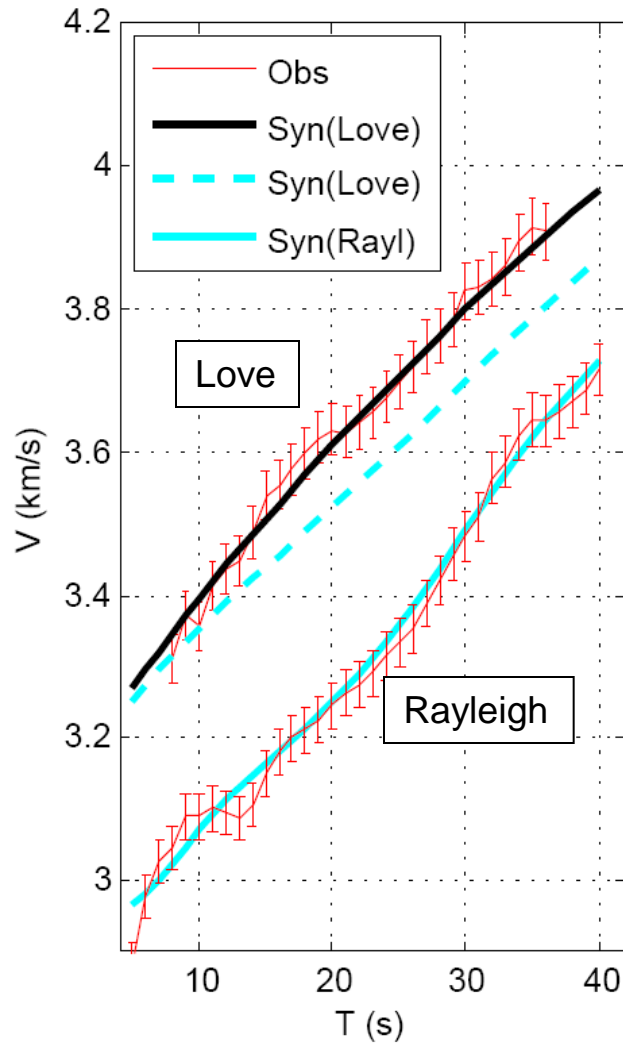
From Stein and Wysession

Radial Anisotropy from joint inversion of Love and Rayleigh wave dispersion (empirical Green's functions for noise correlation).



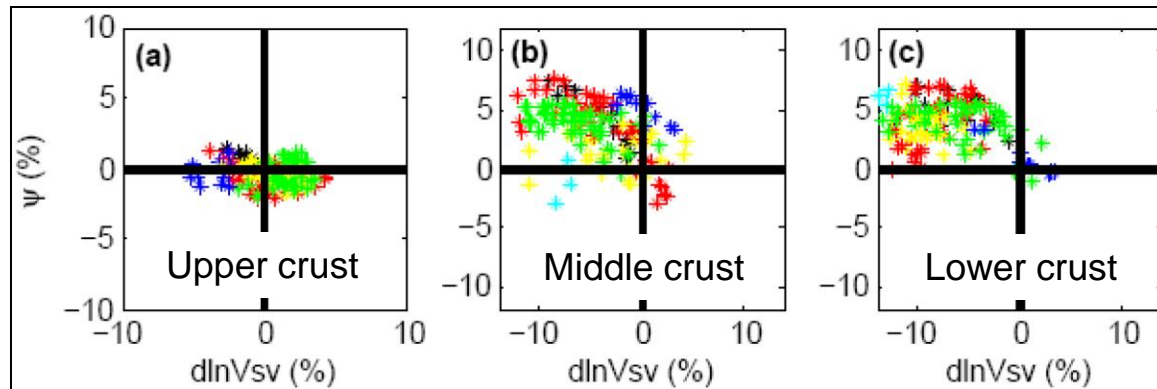
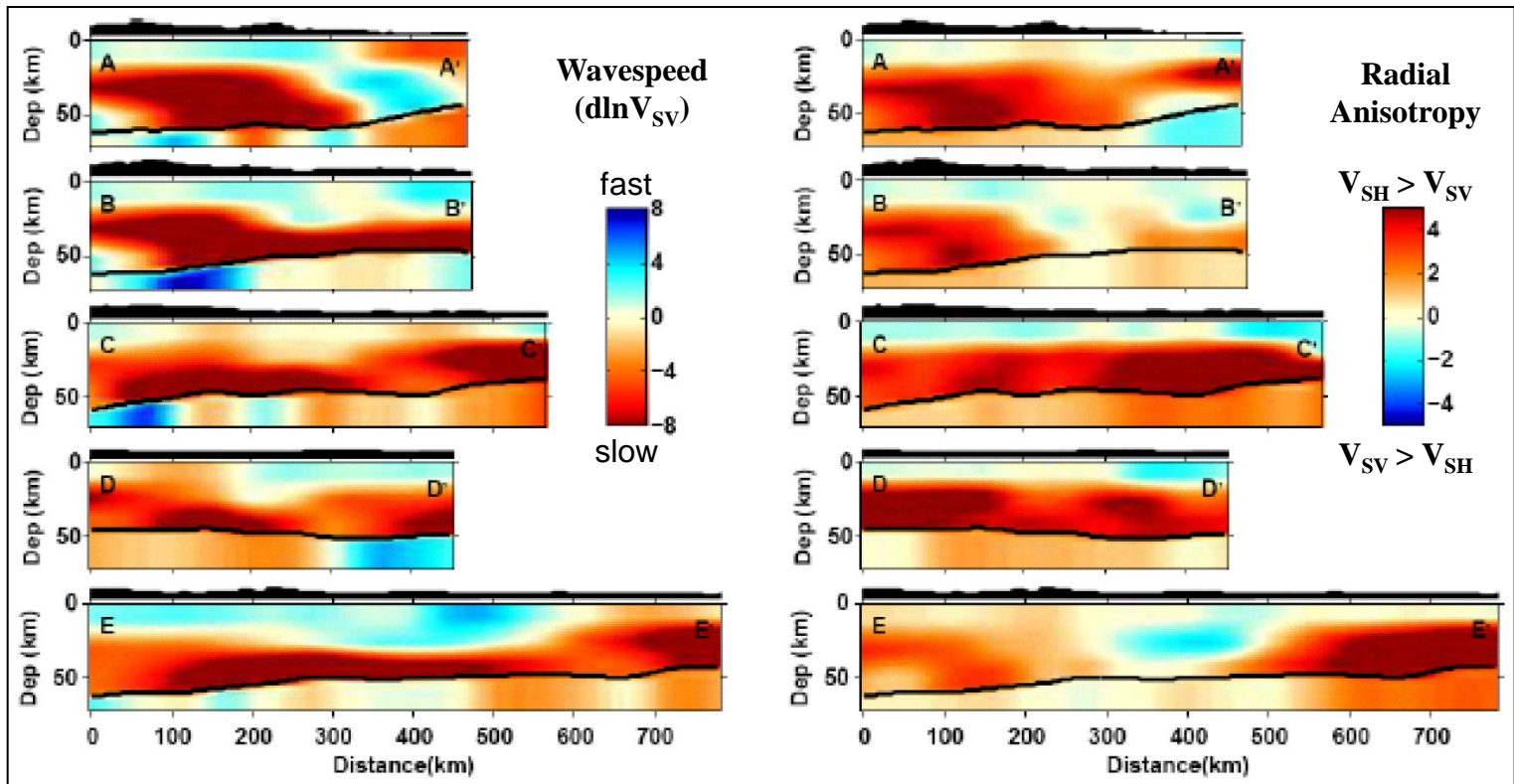
Huang, Yao, and Van der Hilst (GRL, 2010)

Radial Anisotropy (from Love and Rayleigh wave dispersion)



Huang, Yao, and Van der Hilst (GRL, 2010)

Strong correlation with LVZs → horizontal flow in weak zones?



Overview of lecture:

1. Introduction/background

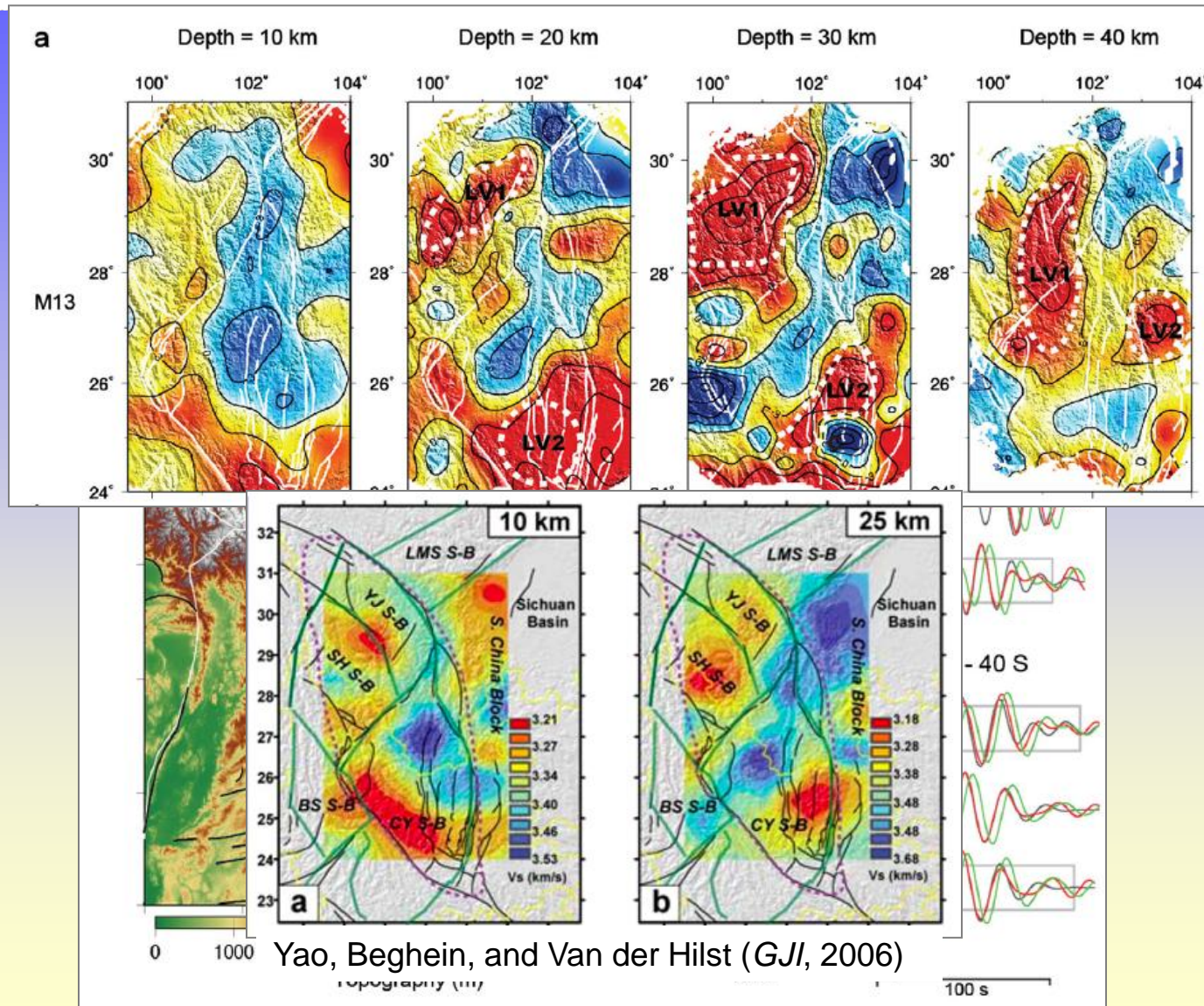
2. Ambient noise and surface wave tomography (MIT, 2005-2015)

- combining ambient noise and earthquake data
- ~~➤ quantifying and correcting for uneven noise distribution~~
- ~~➤ azimuthal anisotropy~~
- radial anisotropy
- **Adjoint tomography with ambient noise data**
- Joint inversion dispersion data and receiver functions

3. Imaging of interfaces

Low wave speed zones in the crust beneath SE Tibet revealed by ambient noise adjoint tomography

Min Chen^{1,2}, Hui Huang¹, Huajian Yao^{1,3}, Rob van der Hilst¹, and Fenglin Niu^{2,4}



Overview of lecture:

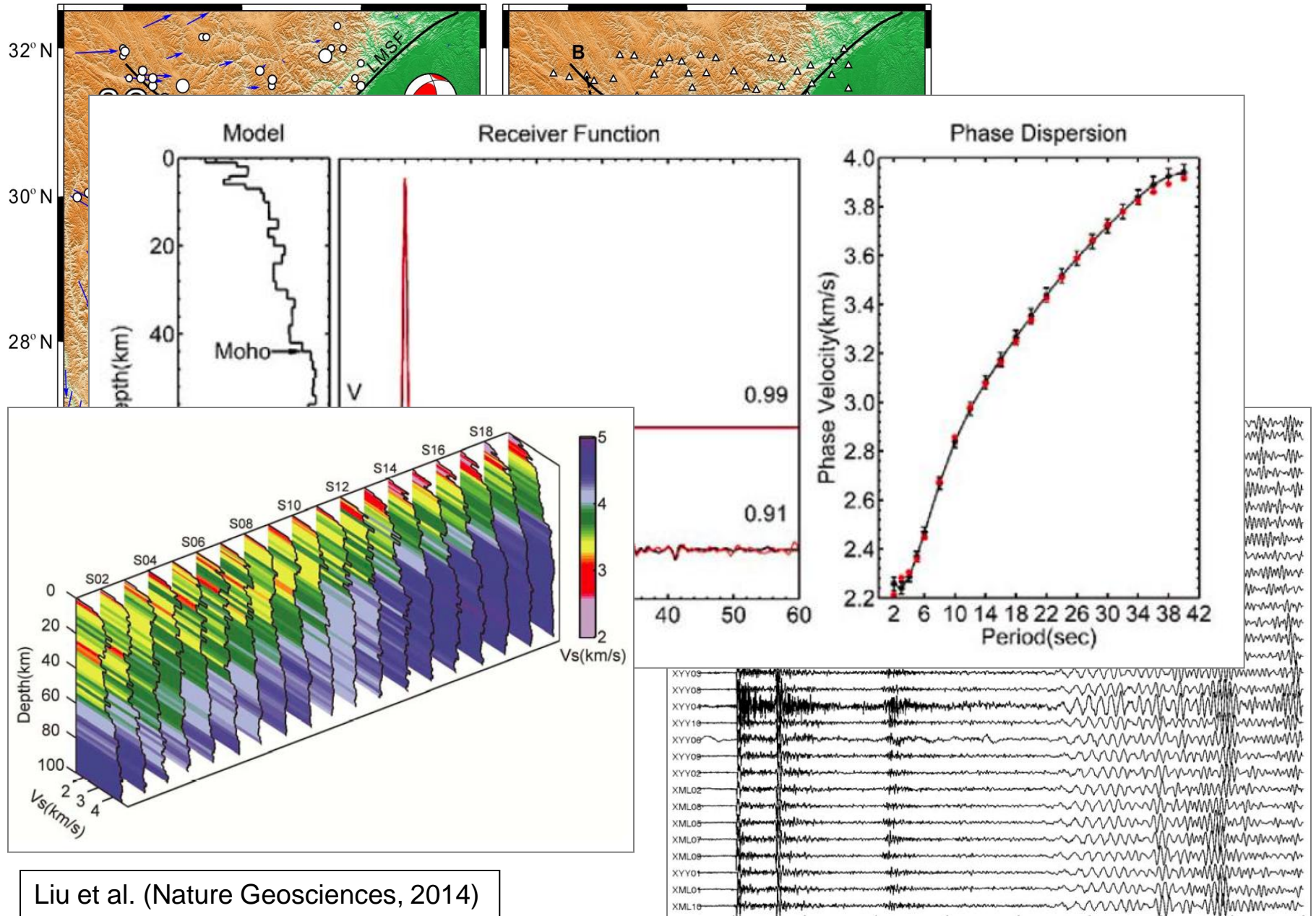
1. Introduction/background

2. Ambient noise and surface wave tomography (MIT, 2005-2015)

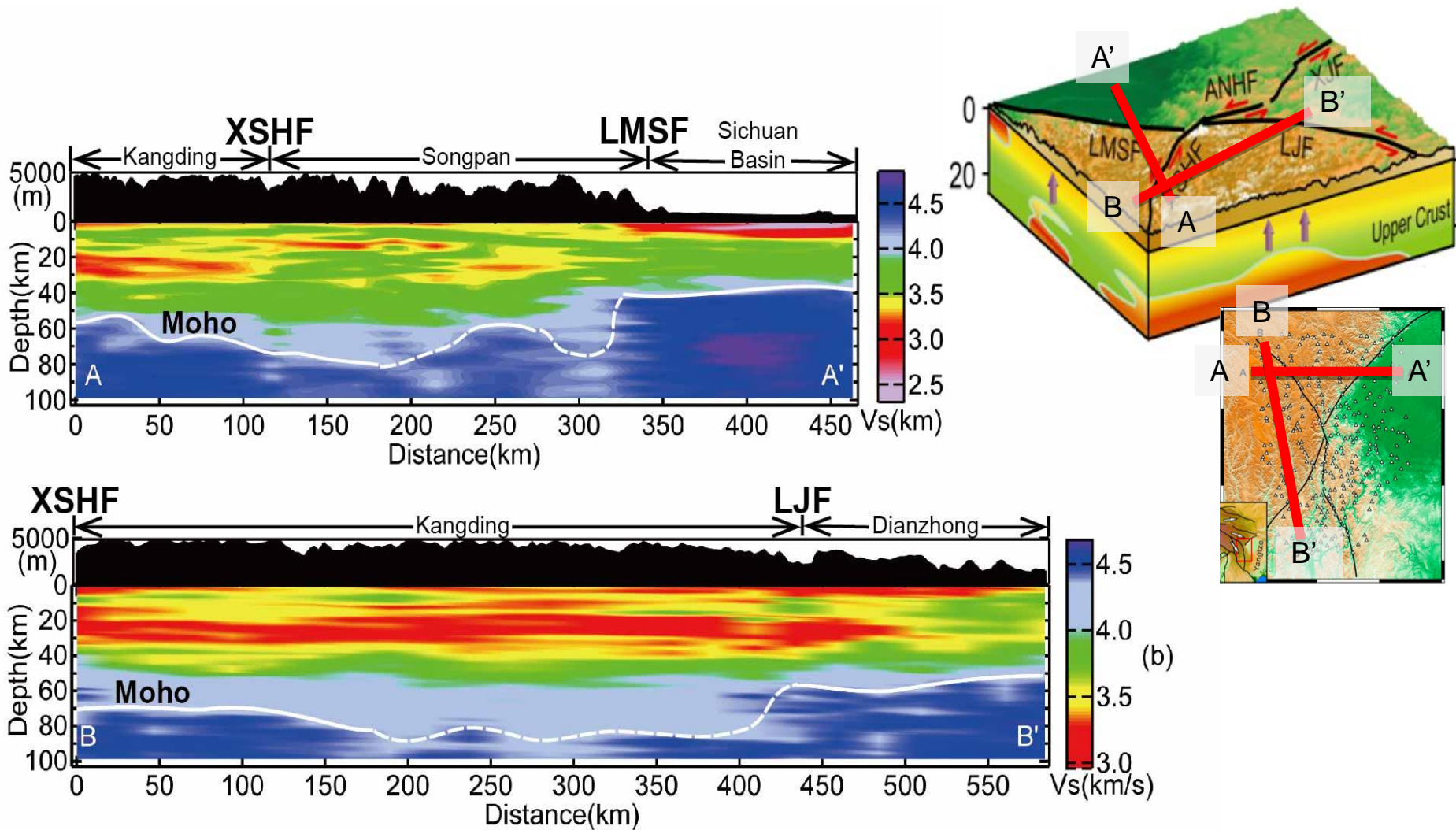
- combining ambient noise and earthquake data
- ~~➤ quantifying and correcting for uneven noise distribution~~
- ~~➤ azimuthal anisotropy~~
- radial anisotropy
- adjoint tomography with ambient noise data
- joint inversion dispersion data and receiver functions

3. Imaging of interfaces

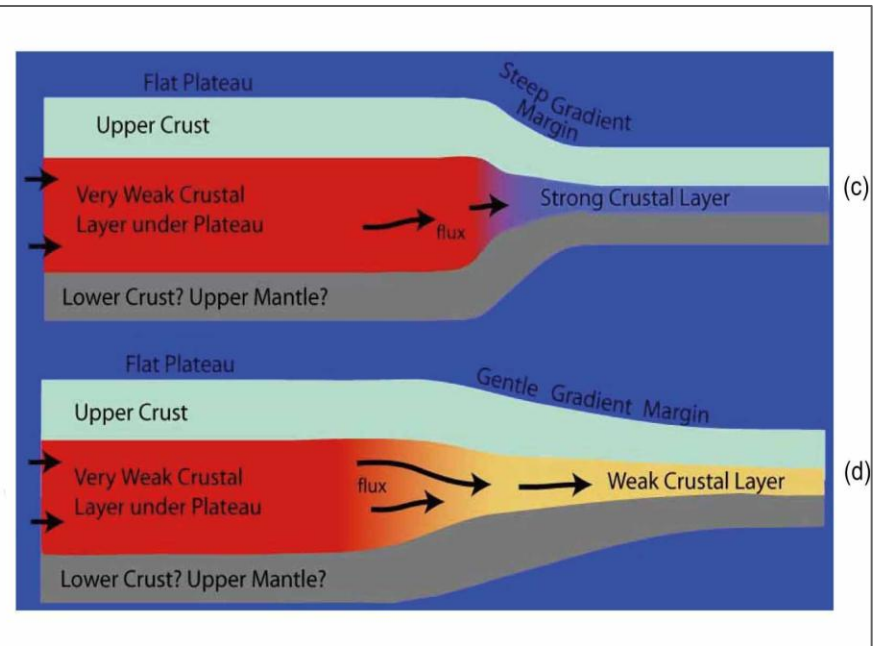
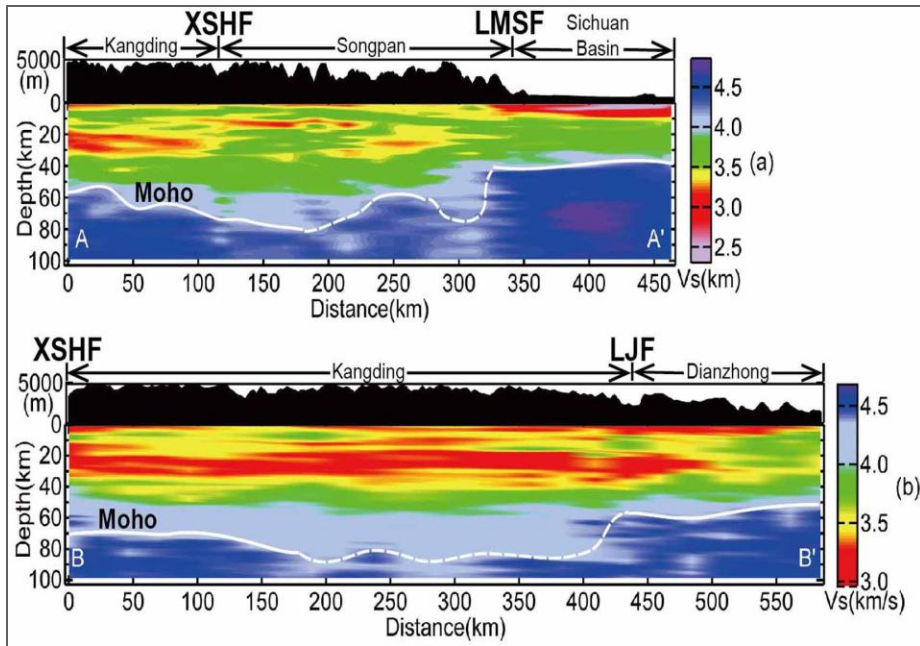
High resolution studies with dense seismograph arrays



Liu et al. (Nature Geosciences, 2014)



Topography and shear wavespeed variations from joint inversion of P-receiver functions and Ambient Noise (Rayleigh wave) Tomography across region of steep relief (A-A'; top) and gentle topographic gradient (B-B'; bottom).



Crustal structure constrained by waveform data obtained by a dense seismography array in western Sichuan.

Concept: canonical channel flow model. (Figure courtesy of L. Royden, MIT).

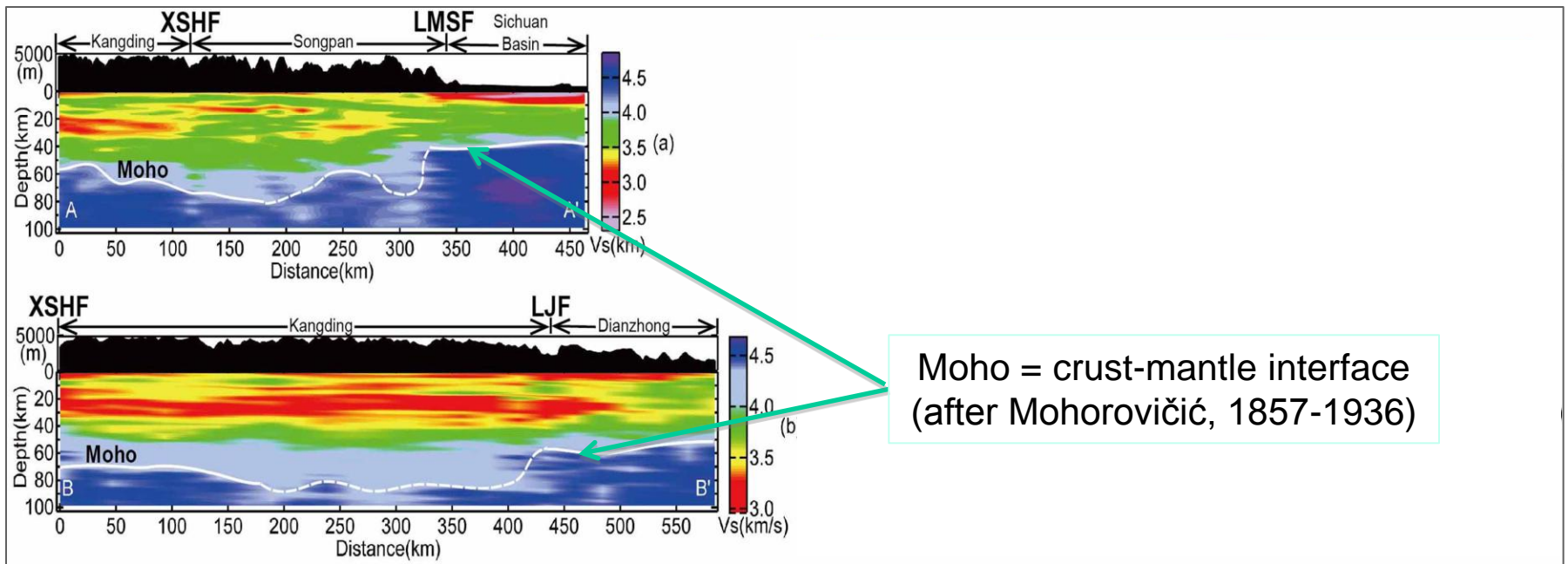
Overview of lecture:

1. Introduction/background

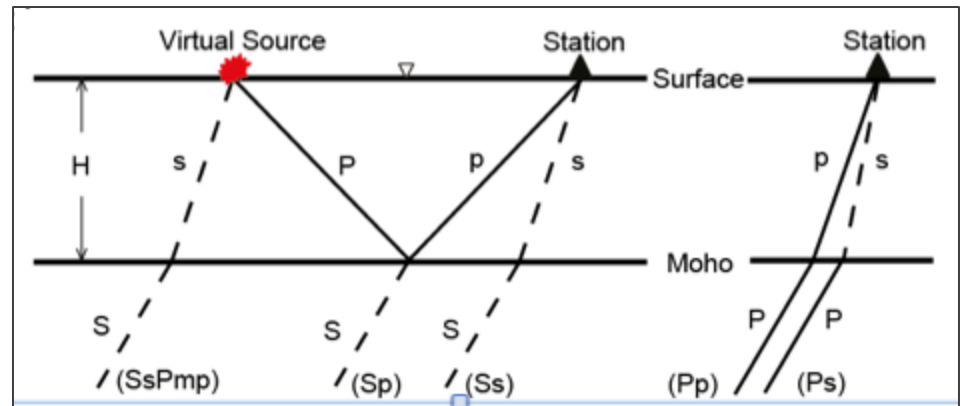
2. Ambient noise and surface wave tomography (MIT, 2005-2015)

- combining ambient noise and earthquake data
- ~~➤ quantifying and correcting for uneven noise distribution~~
- ~~➤ azimuthal anisotropy~~
- radial anisotropy
- adjoint tomography with ambient noise data
- joint inversion dispersion data and receiver functions

3. Imaging of interfaces

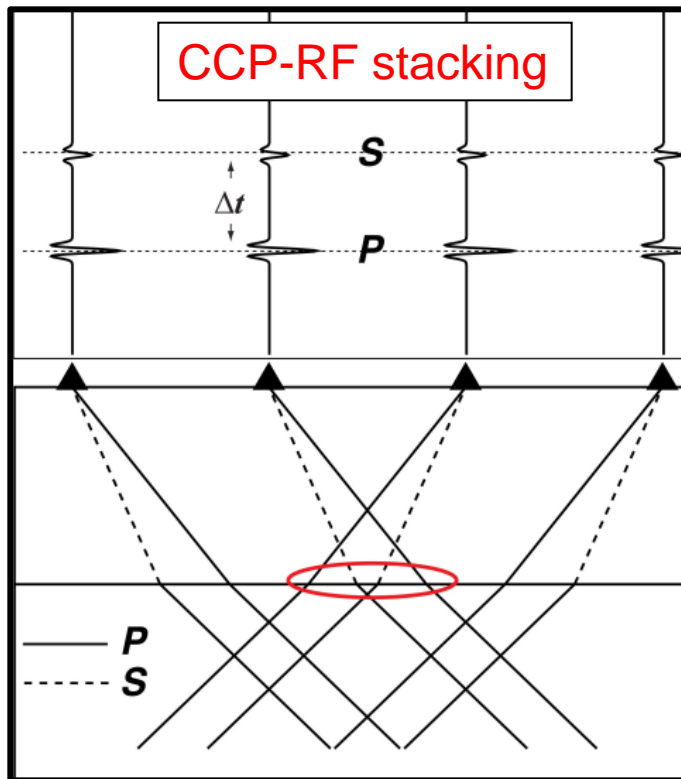


Imaging of the Moho with Converted Waves (*P-to-S* or *S-to-P*)



Yu et al.(EPSL, 2012)

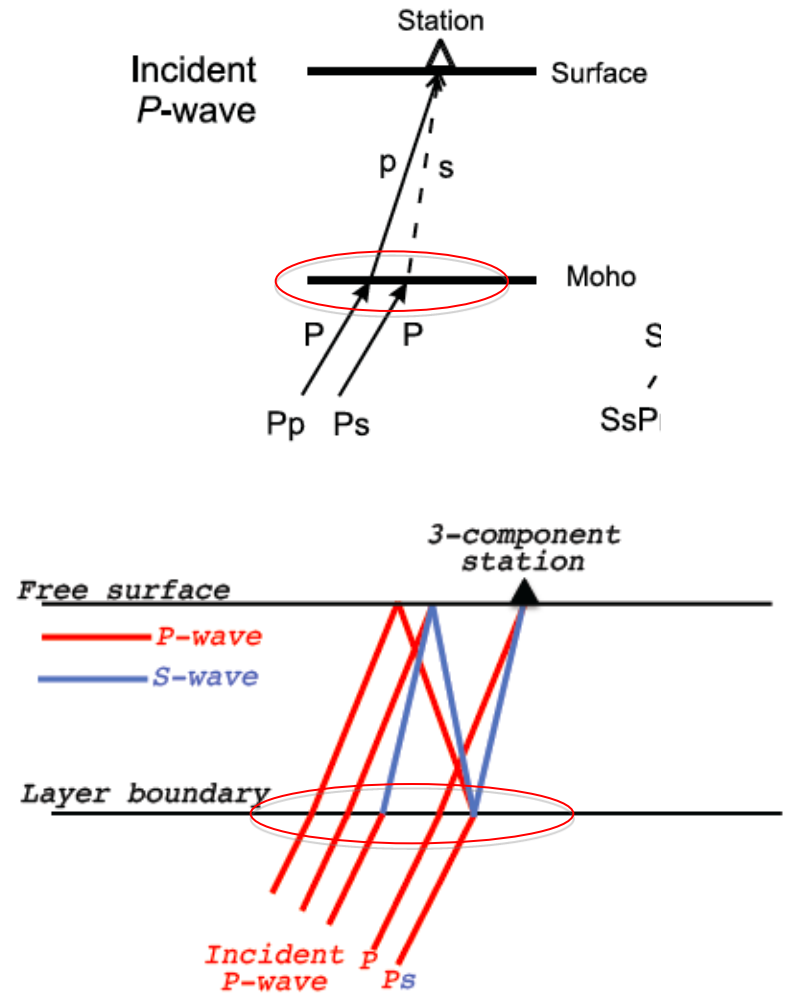
Traditional approach (concept)



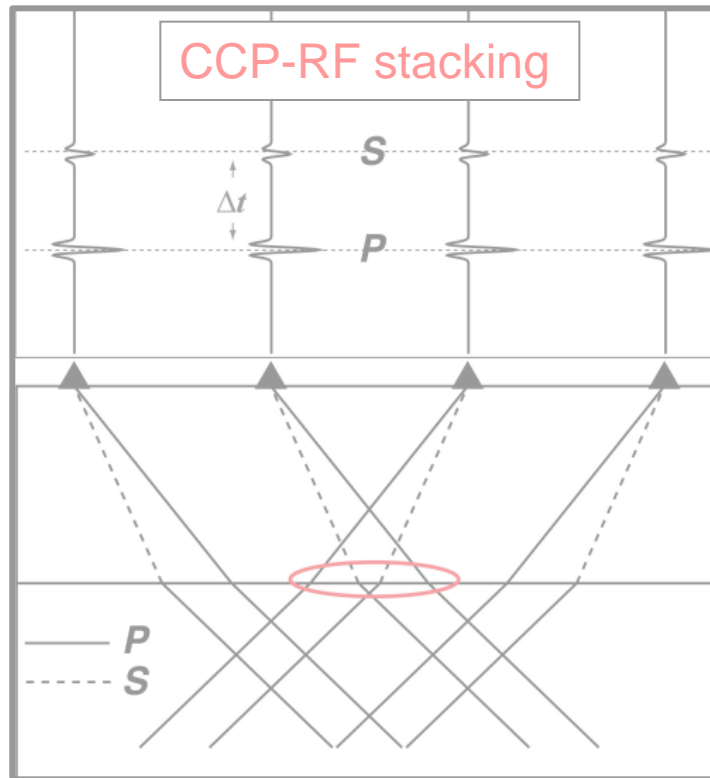
Common **C**onversion **P**oint
stacks of converted waves
(**R**eceiver **F**unctions):

- Time differences mapped directly to depth
- **Horizontal interfaces**

Imaging with converted waves



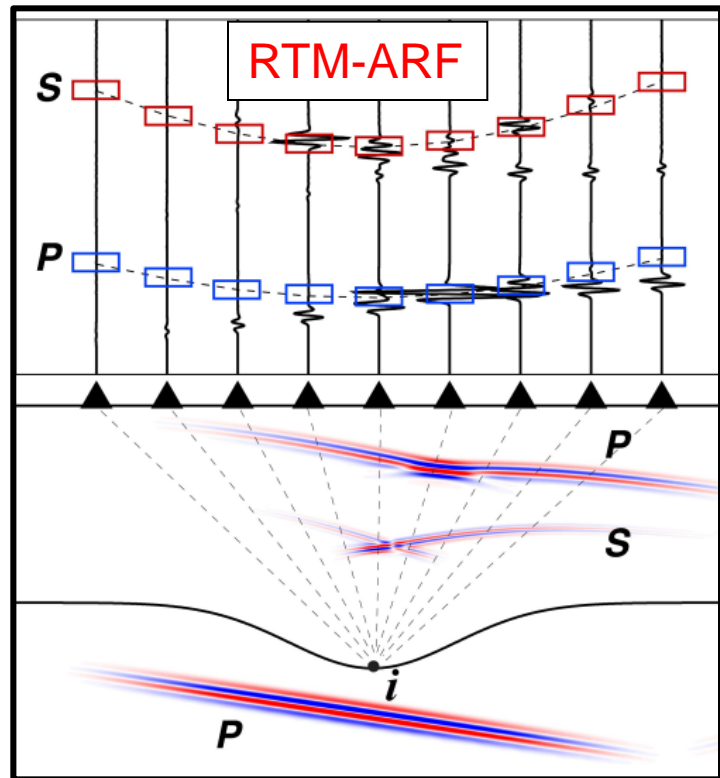
Traditional approach (concept)



Common **C**onversion **P**oint
stacks of converted waves
(**R**eceiver **F**unctions):

- Time differences mapped directly to depth
- Horizontal interfaces

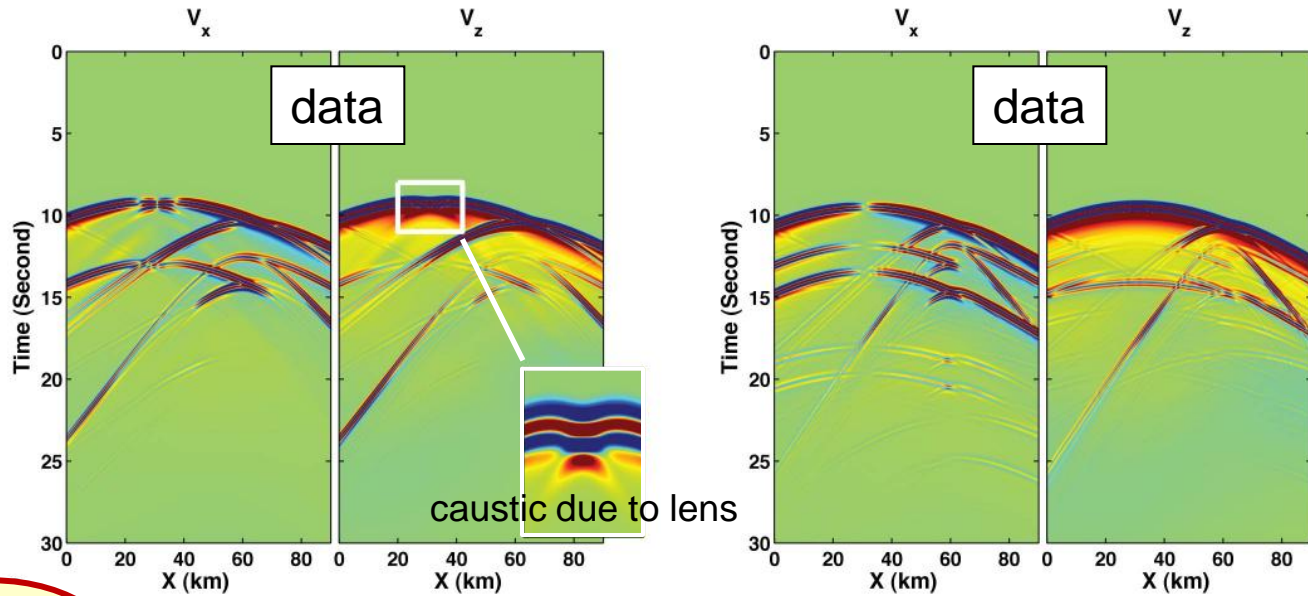
Shang et al. (GRL, 2012)



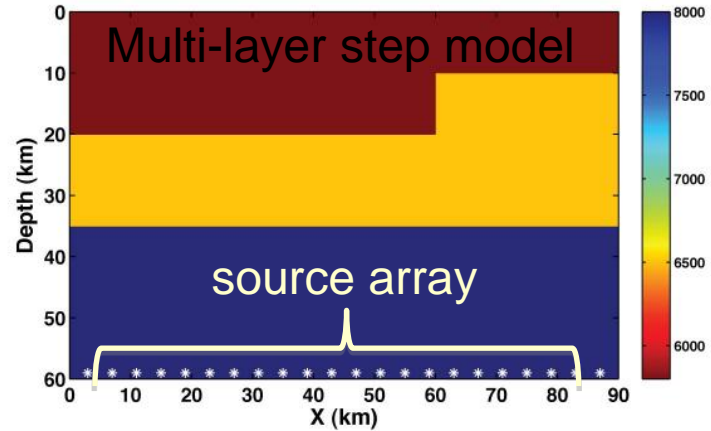
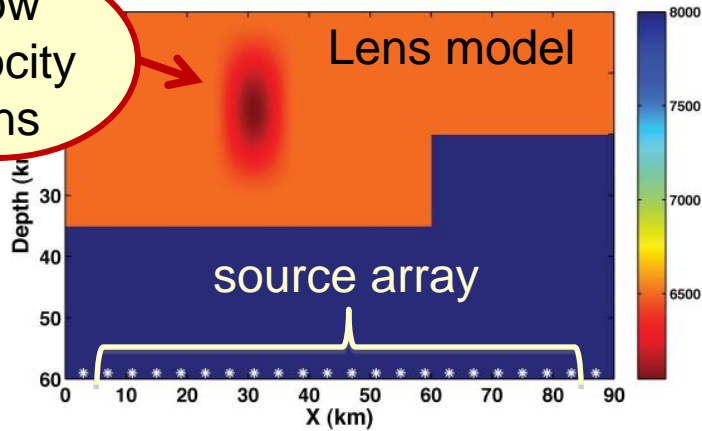
Reverse **T**ime **M**igration of
Array **R**eceiver **F**unctions:

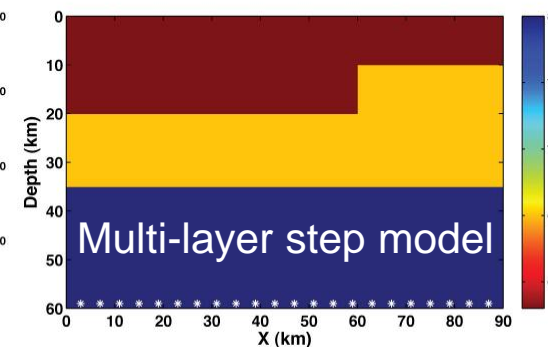
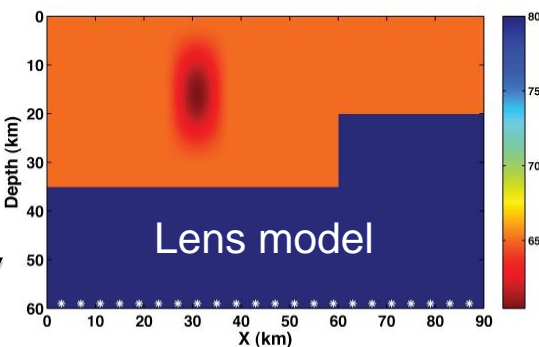
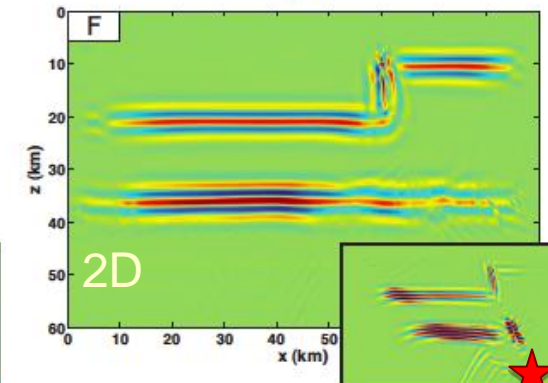
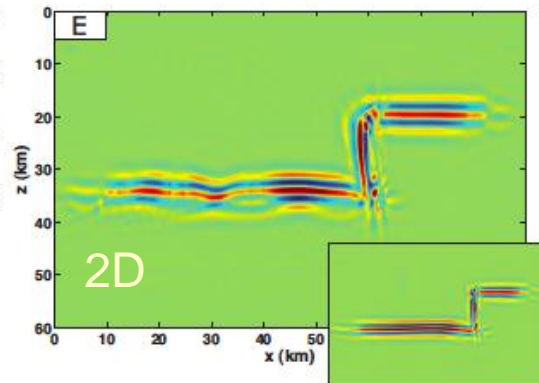
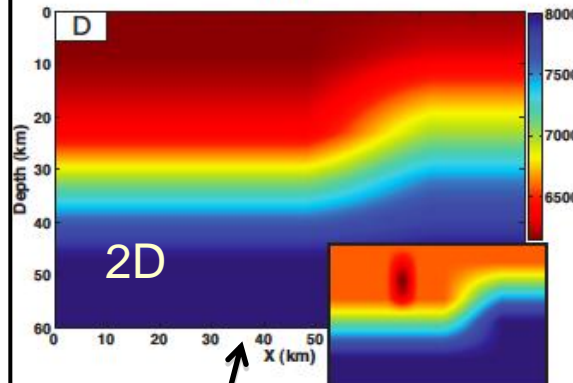
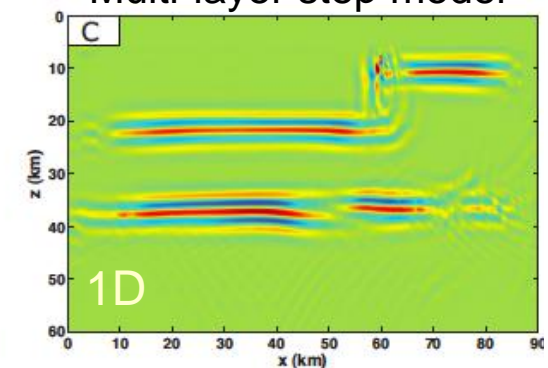
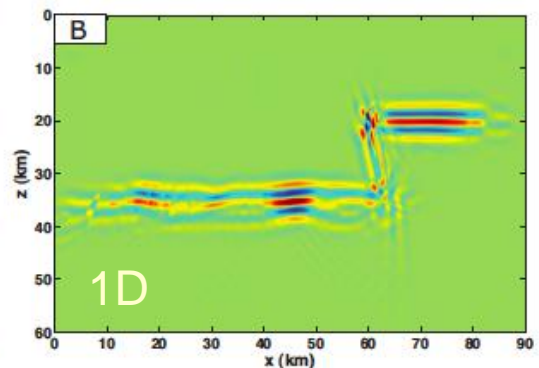
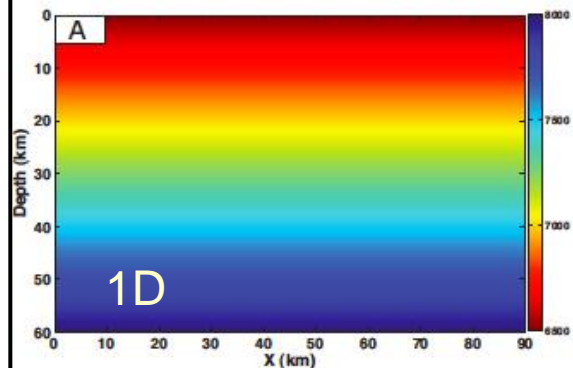
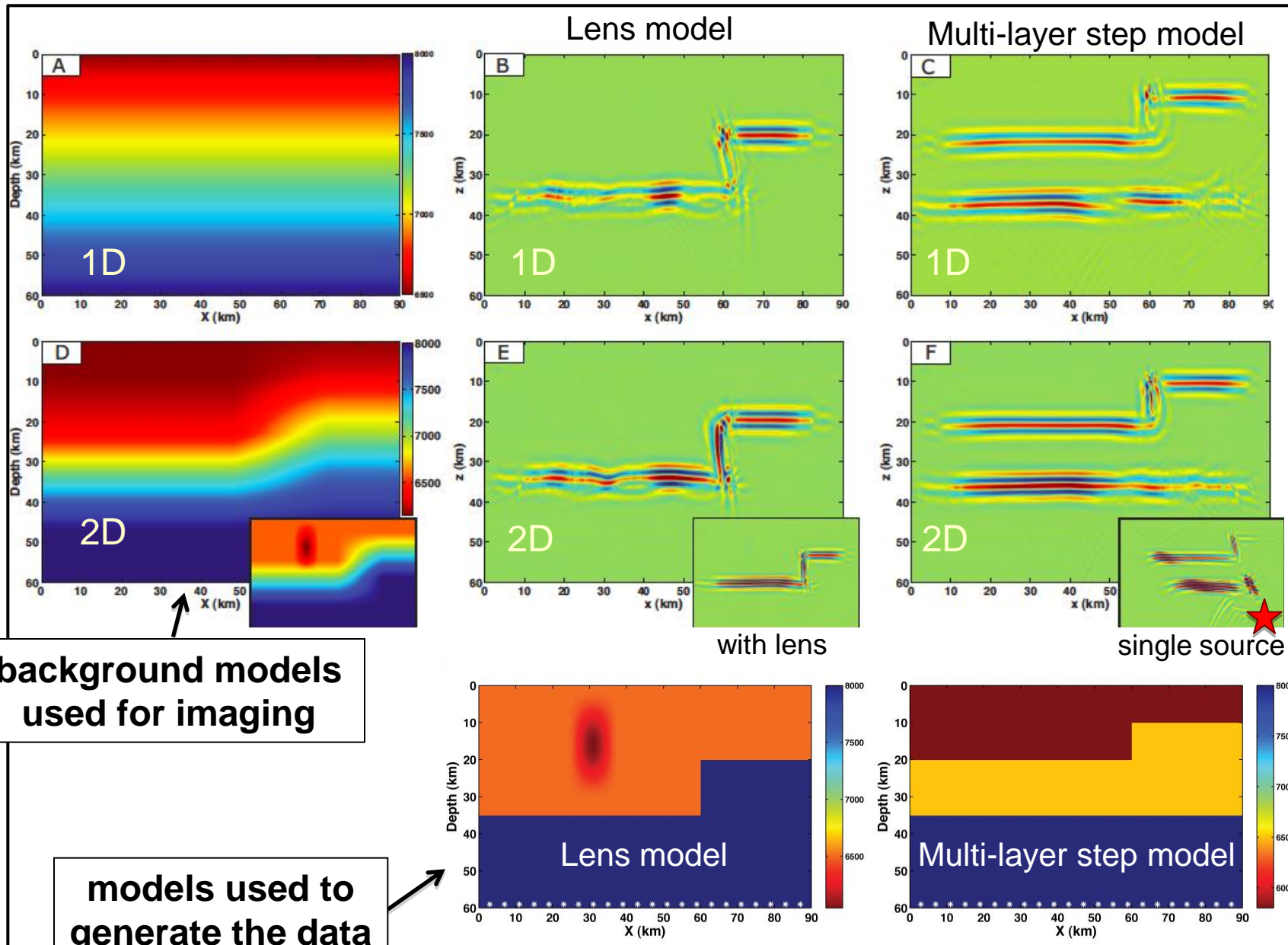
- Cross-correlations: incoming & time reversed and *P* & *S* waves (“imaging condition“)
- No assumption on structure

Synthetic experiments for two test models



Low velocity lens





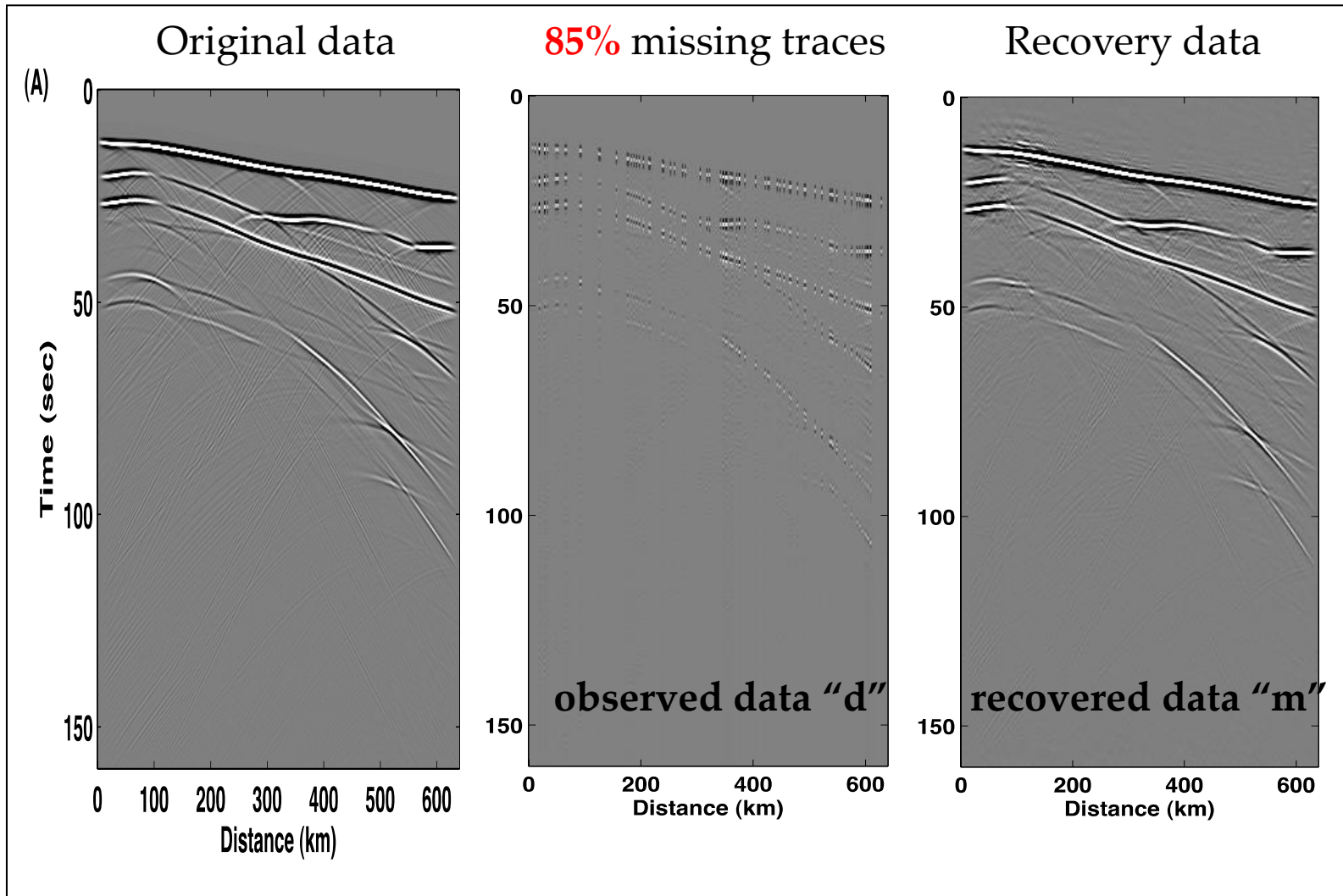
background models used for imaging

models used to generate the data

Promising but ...

... important practical considerations:

- Need good starting model (2- or 3D structure, e.g., from ambient noise or wave equation reflection tomography)
- Need to have densely sampled wavefield (preferably on a regular grid) → not always available → need interpolation → wave field *continuation*



Wave field continuation

Sparsity Promoting Interpolation

$$\mathbf{d} = \mathbf{G}\mathbf{m} + \mathbf{n}$$

d: observed data
m: recovered
 (interpolated) data
G: sampling operator
n: noise

$$\mathbf{m} = \mathbf{C}^T \mathbf{x}$$

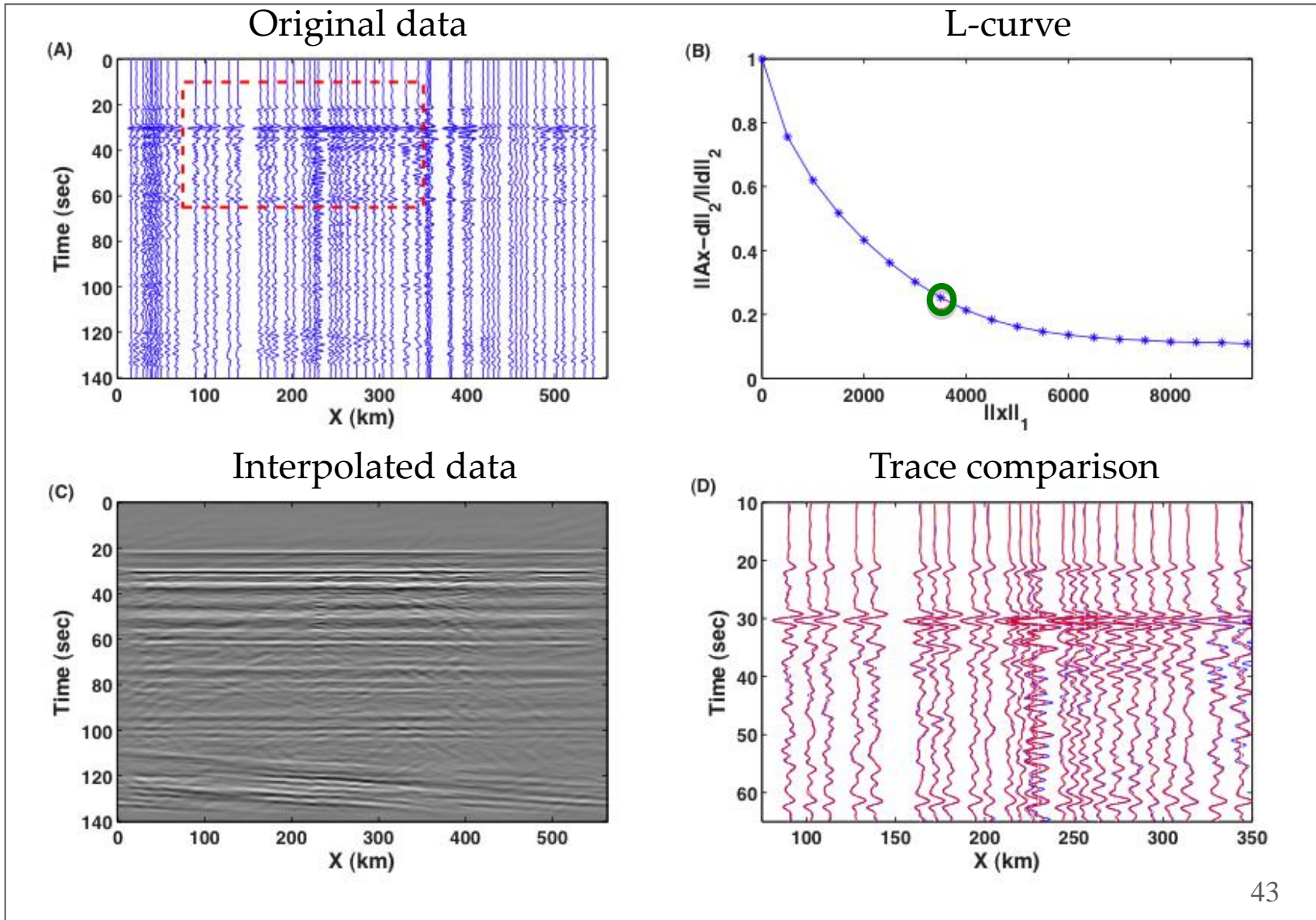
$$\mathbf{A} = \mathbf{G}\mathbf{C}^T$$

x: curvelet coefficients
C^T: inverse curvelet
 transform

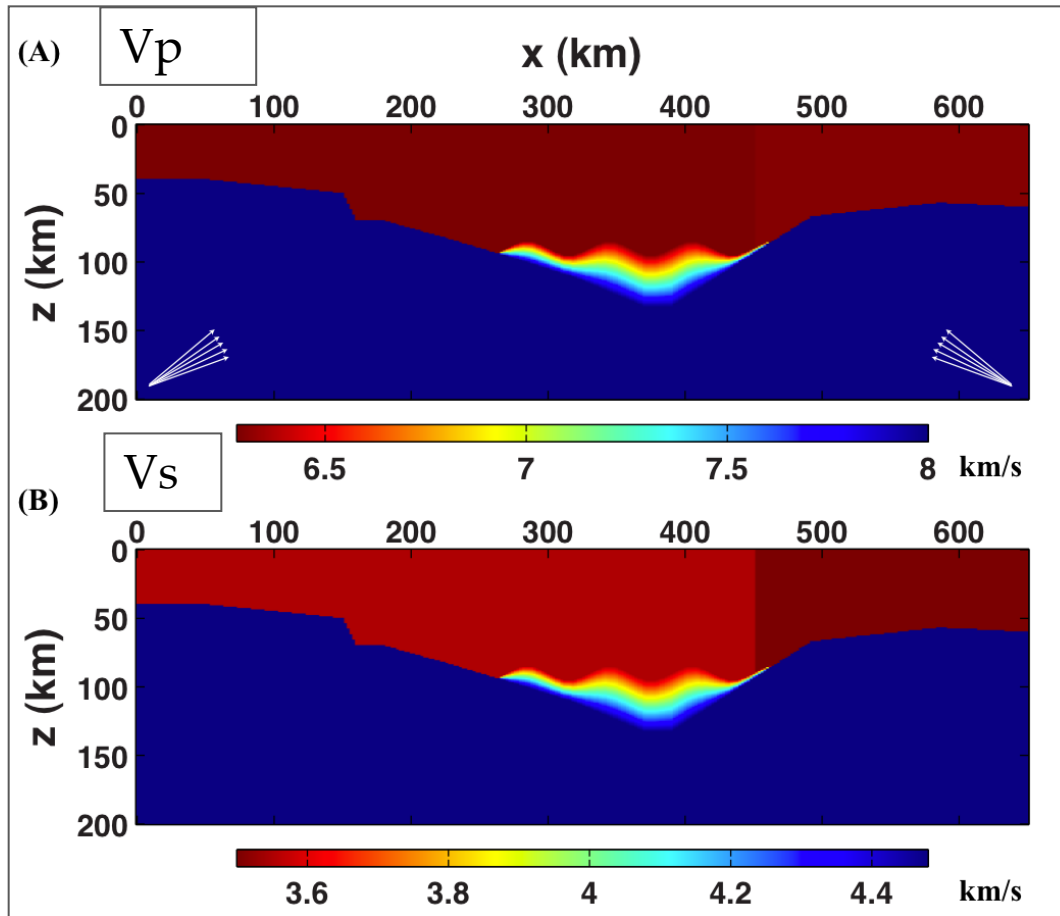
Minimize

$$J = \frac{1}{2} \|\mathbf{d} - \mathbf{A}\mathbf{x}\|_2^2 + \lambda \|\mathbf{x}\|_1$$

Real Data Example

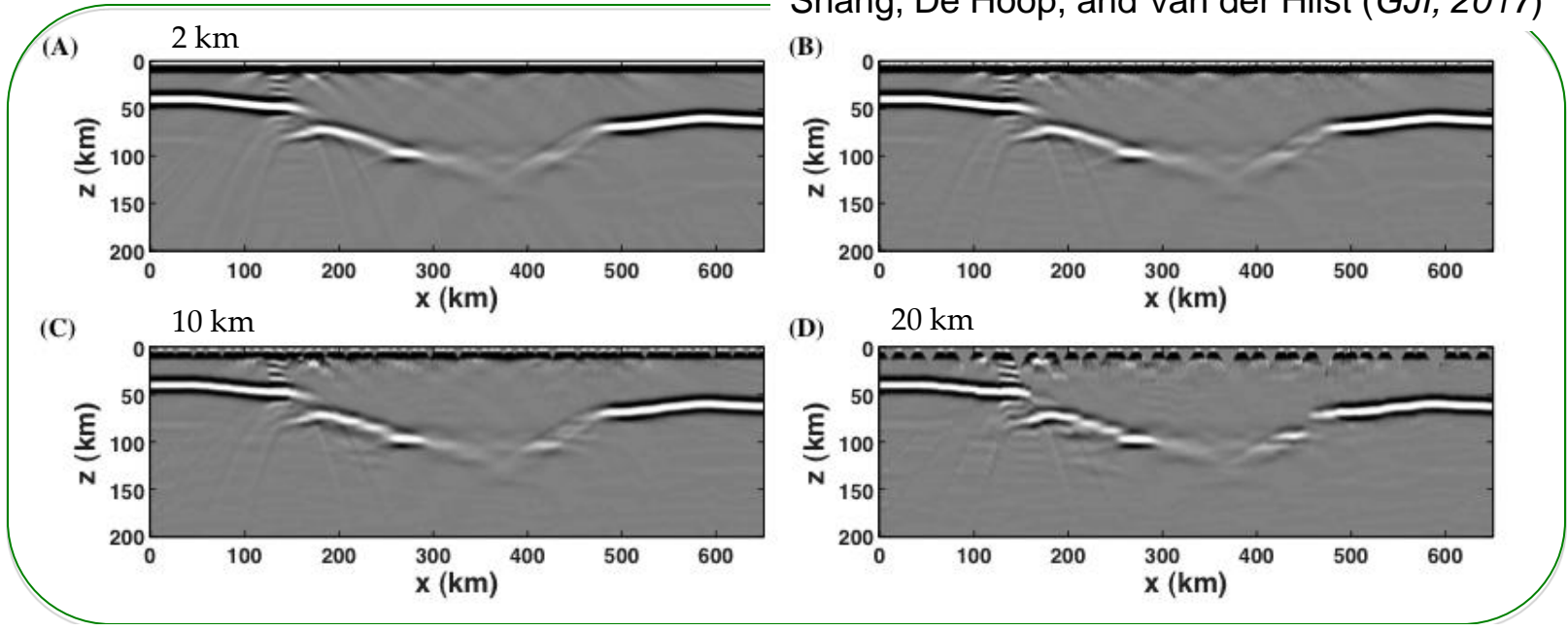


Application to Sparsely Sampled Synthetic data

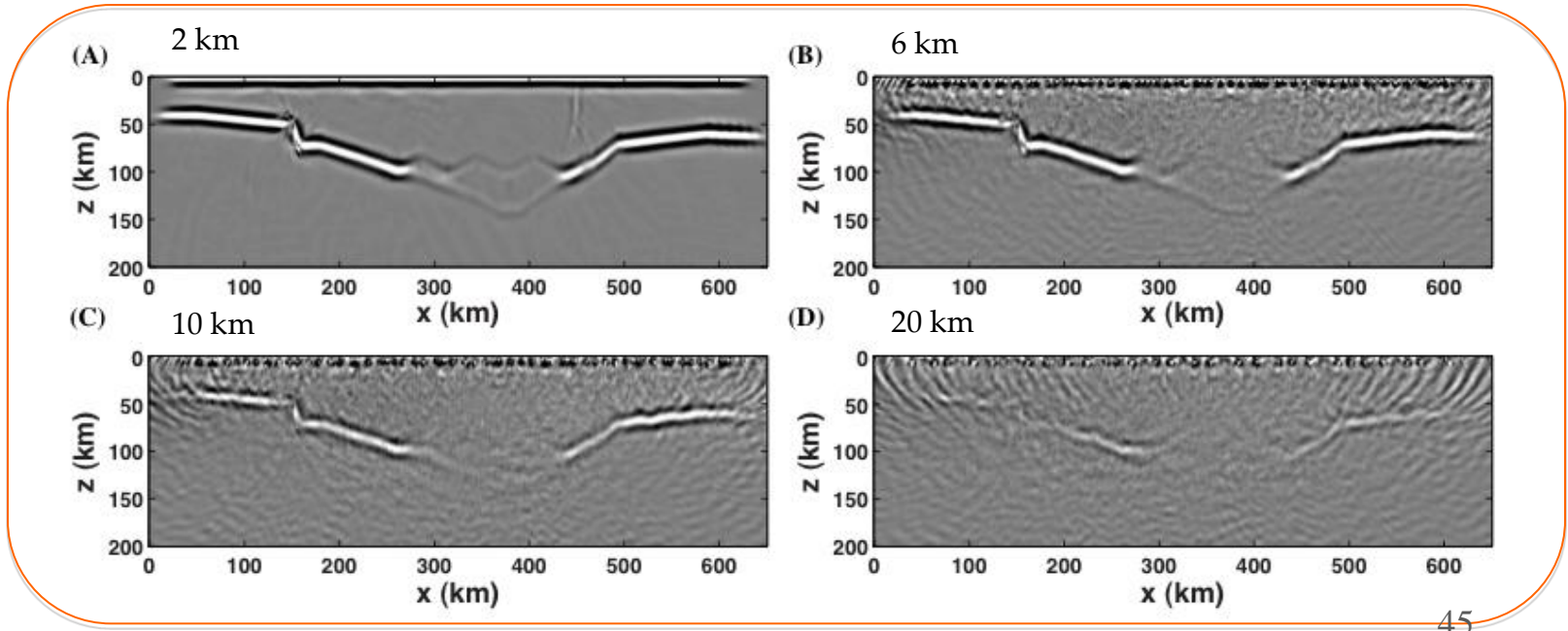


- 10 plane P waves (incident angle: 20~40 degree)
- Source central frequency: 0.5 Hz
- Station interval: 2, 6, 10 and 20 km

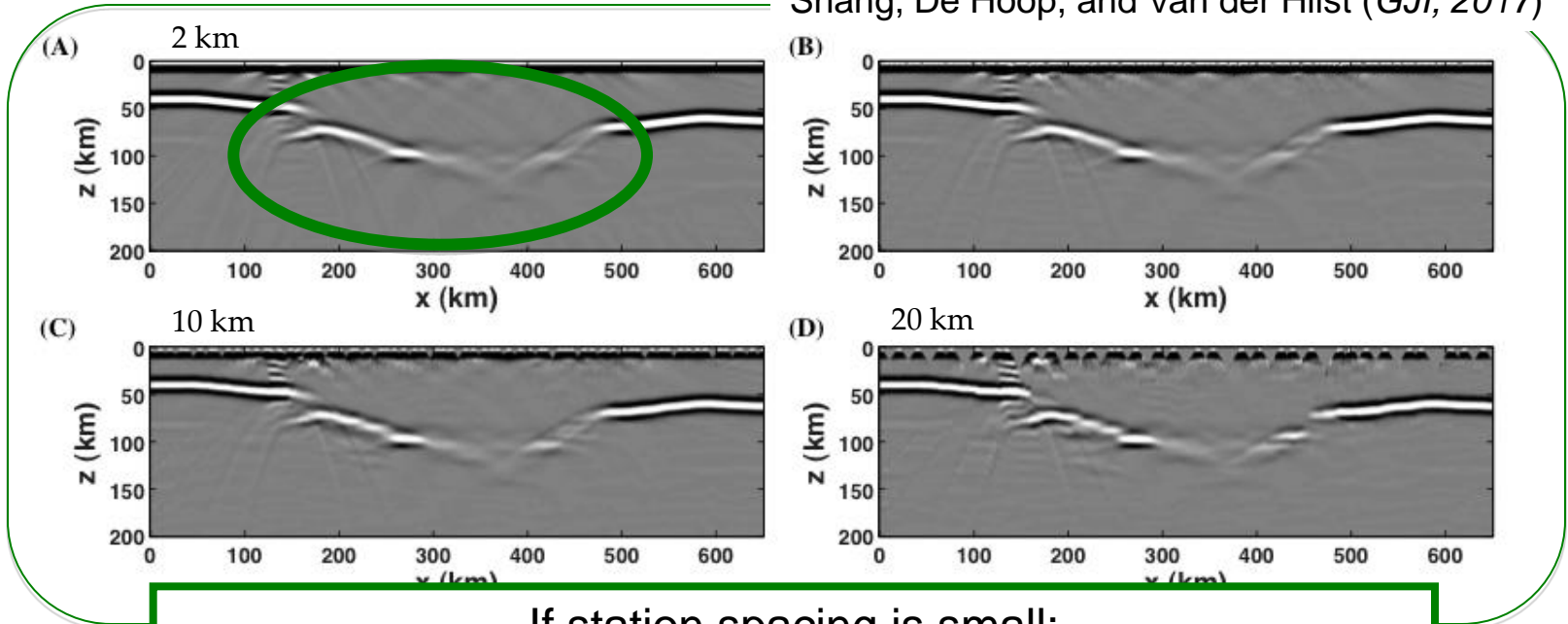
CCP



RTM
without
interp

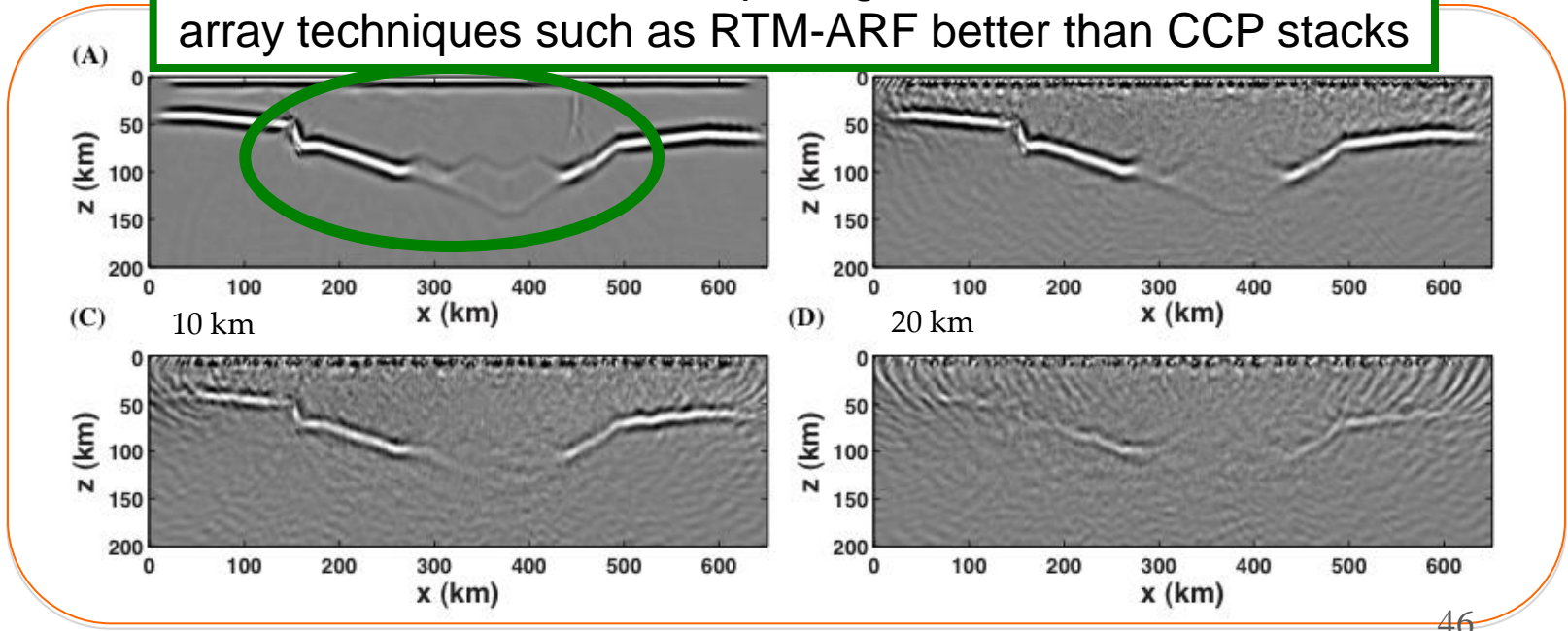


CCP

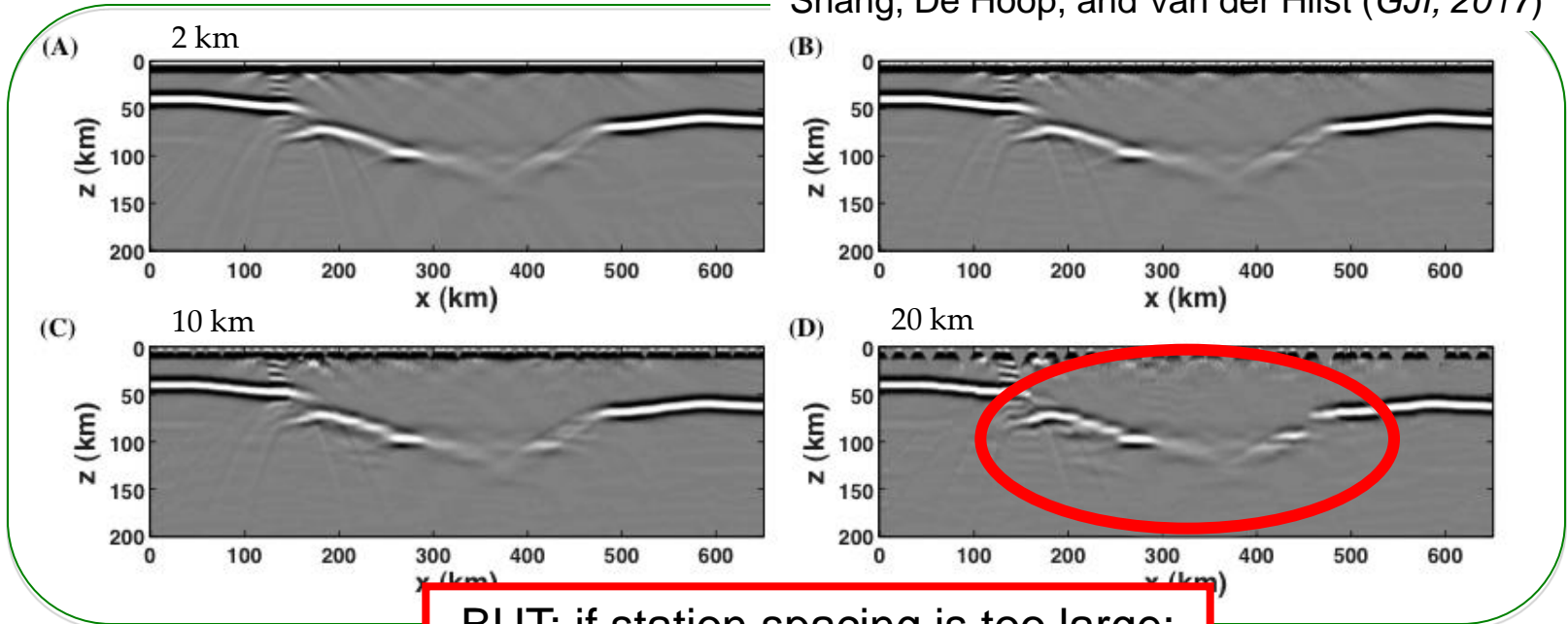


If station spacing is small:
array techniques such as RTM-ARF better than CCP stacks

RTM
without
interp

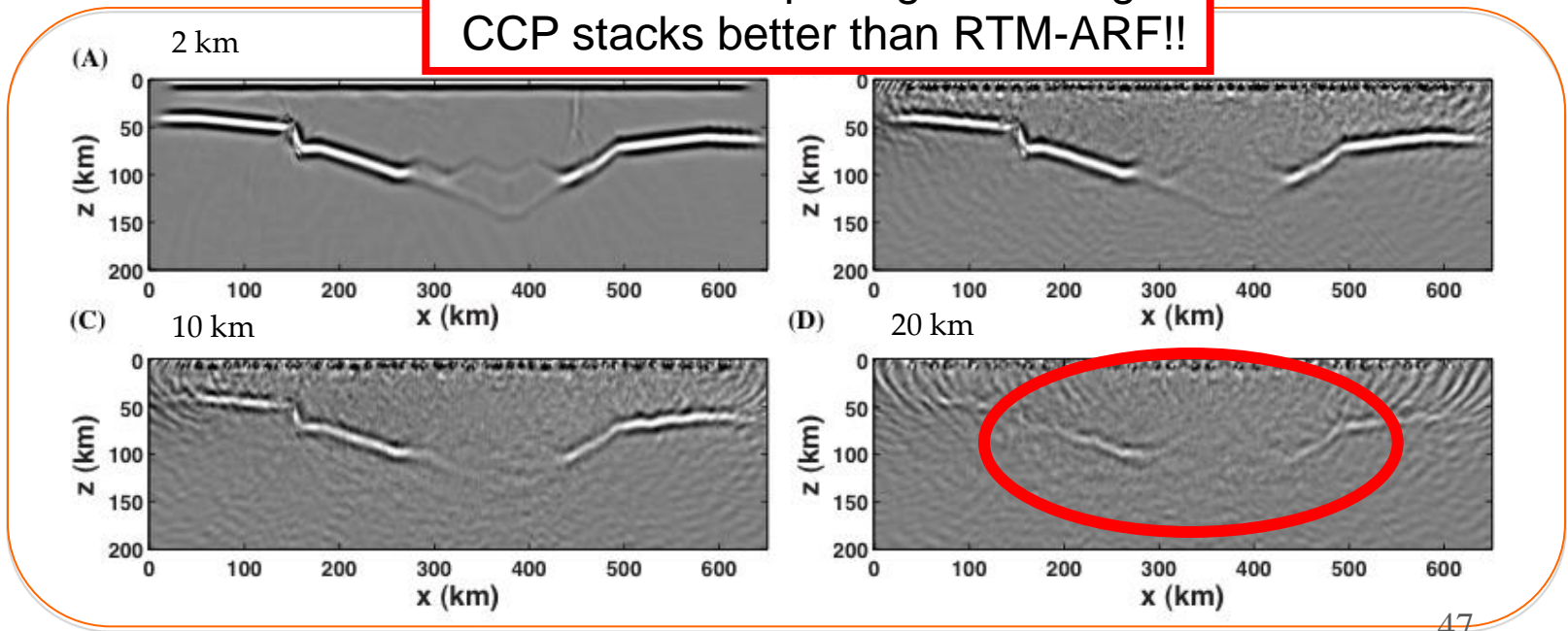


CCP

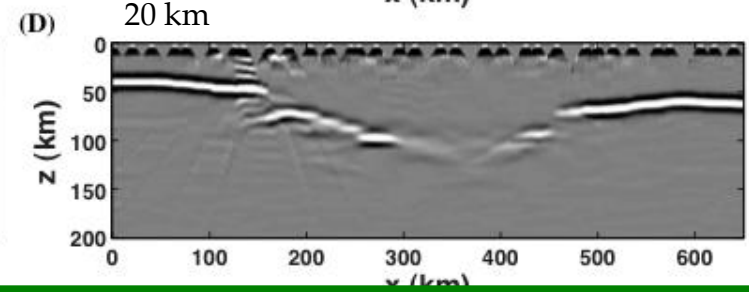
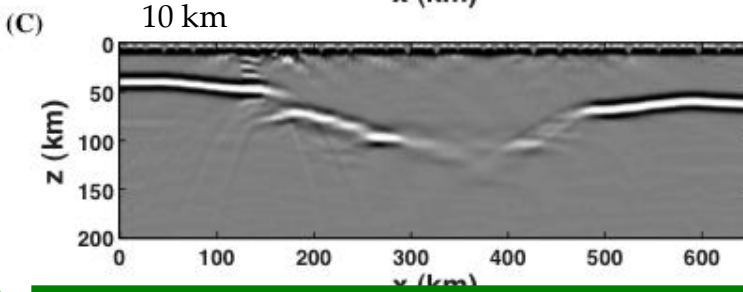
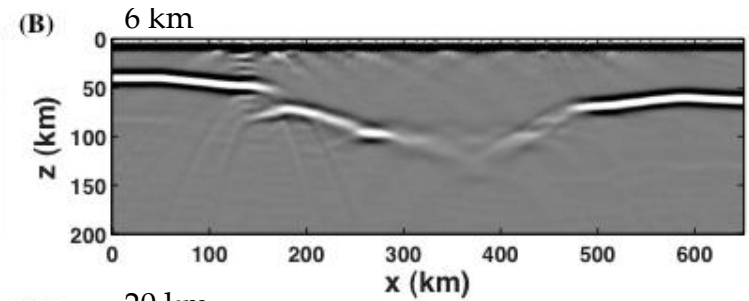
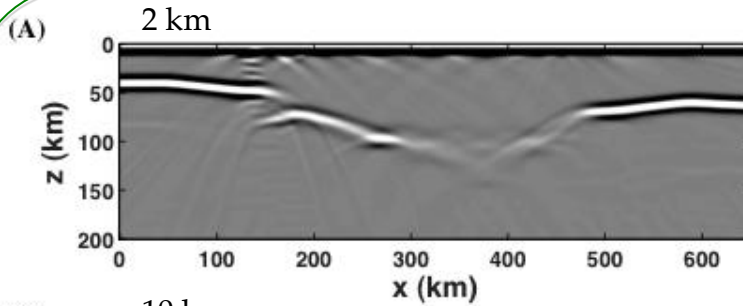


**BUT: if station spacing is too large:
CCP stacks better than RTM-ARF!!**

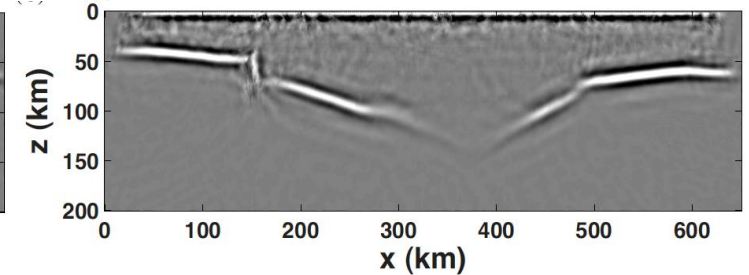
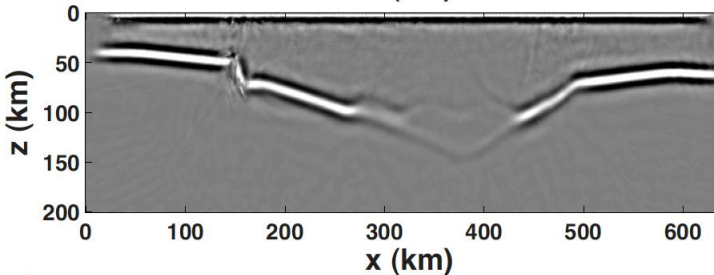
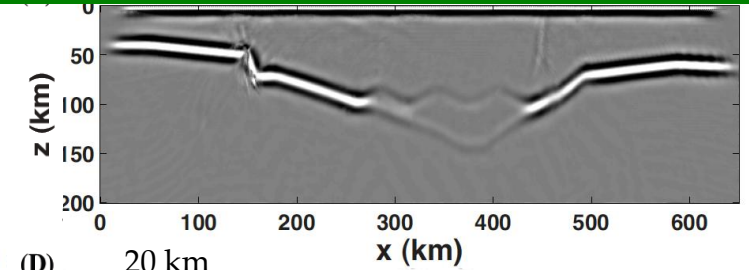
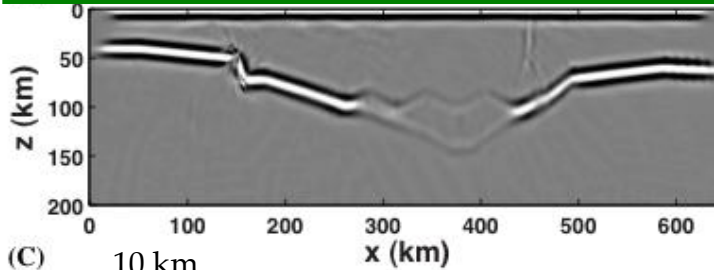
RTM
without
interp



CCP

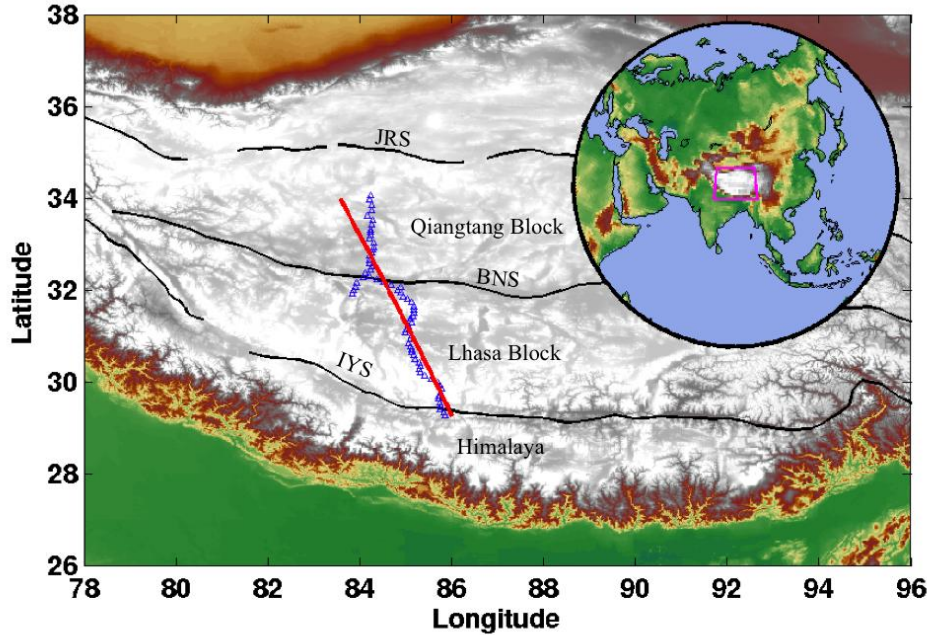


With interpolation/data continuation:
array techniques such as RTM-ARF always better than CCP stacks



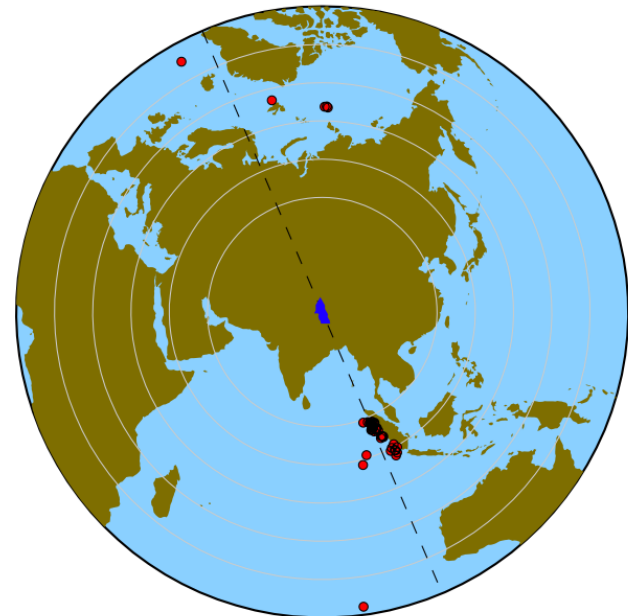
RTM
after
interp

Application to Hi-CLIMB data – Preliminary Result

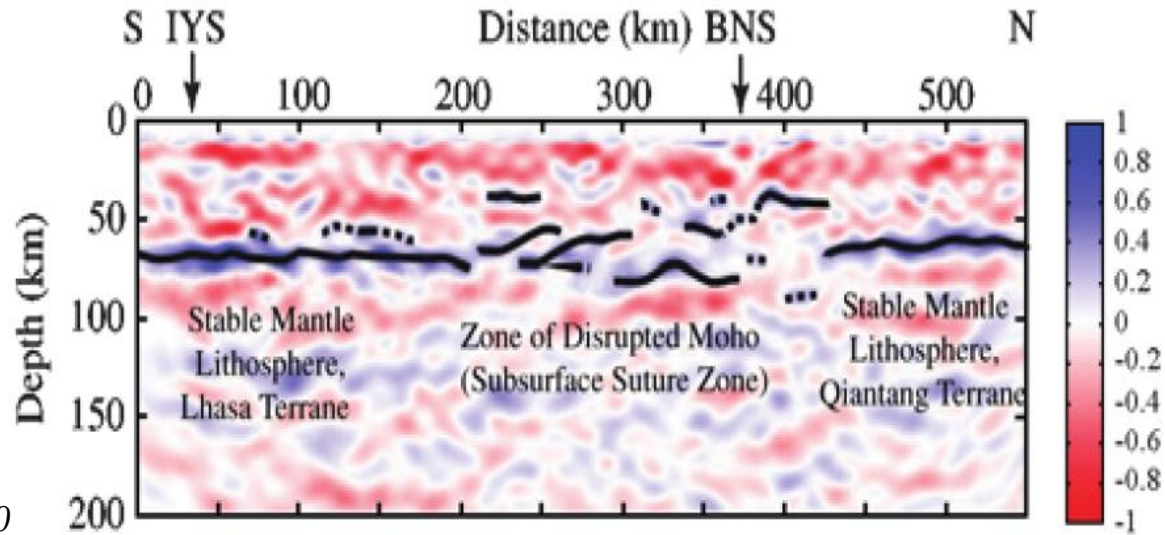


- 71 stations
- Station spacing: 2~40 km
average interval: 10 km

- 75 events, 70 from SE, 5 from NW
- Epicentral-distance: 30~80 degree

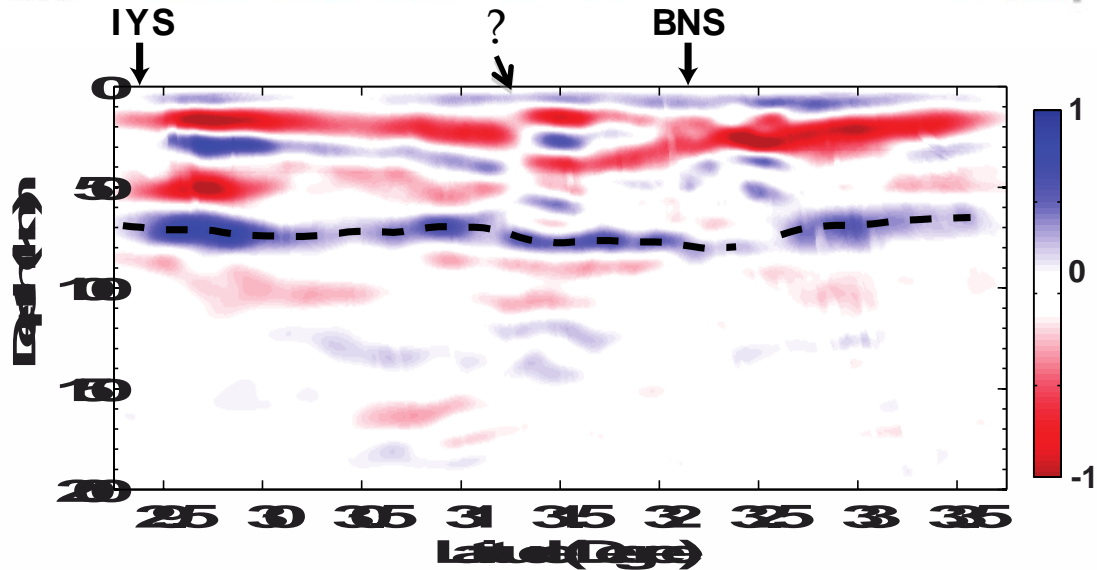


Gaussian beam migration

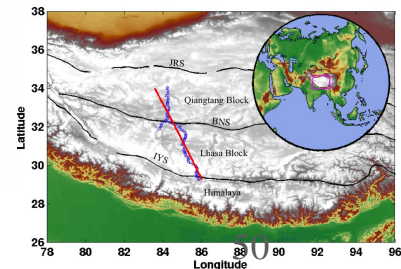


Nowack et al. 2010

RTM



Shang et al. (2014)



Some conclusions:

- Complex structures → underlying assumptions limit resolution and accuracy → just adding stations (and reducing station spacing) gives diminishing returns!!
- Need better imaging methods to make the best use of dense array data → array methods, like reverse time migration (RTM) → Ideal spacing depends on frequency and depth of target (2-5 km for crustal imaging).
- But: Need powerful data–preprocessing to enable application of RTM type techniques in earthquake seismology (to mitigate effects of uneven sampling).
- Without such pre-processing, conventional (single-station) methods may work better than array methods on poorly sampled data.



Thank You

